bioRxiv preprint first posted online Nov. 5, 2018; doi: http://dx.doi.org/10.1101/461947. The copyright holder for this preprint (which was not peer-reviewed) is the author/funder, who has granted bioRxiv a license to display the preprint in perpetuity.
It is made available under a CC-BY-NC-ND 4.0 International license.

Short title: Transcriptomic response to divergent selection

Transcriptomic response to divergent selection for flowering time in maize reveals convergence and key players of the underlying gene regulatory network[1]

Maud Irène Tenaillon[a, 2], Khawla Sedikki[a], Maeva Mollion[a], Martine Le Guilloux[a], Elodie Marchadier[a], Adrienne Ressayre[a], Christine Dillmann[a]

[a] : Génétique Quantitative et Evolution – Le Moulon, Institut National de la Recherche agronomique, Université Paris-Sud, Centre National de la Recherche Scientifique, AgroParisTech, Université Paris-Saclay, F-91190 Gif-sur-Yvette, France

One sentence summary: Experimental evolution in maize inbred lines uncovers determinants of the response to selection and convergence of gene expression.

M.I.T. and C.D. conceived the project and formulated the research plan; M.I.T, A.R. and C.D. supervised the experiments; M.L.G. provided technical assistance; K.S., M.M. set up the pipeline for the analyzes. M.I.T. and C.D. performed the data analyses; C.D. and E.M. helped with data analyzes and interpretations; M.I.T. and C.D. wrote the article with inputs from all the authors.

[1]: This work was supported by a grant overseen by the French National Research Agency (ANR) as part of the “Investments d’Avenir” Programme (LabEx BASC; ANR-11-LABX-0034) to C.D, as well as a grant from Institut de la Recherche Agronomique to A.R. (StaterFS2015-BAP-UMR320-FloSeq); M.M. was financed by GQE-Le Moulon and K.S. by Institut Diversité, Ecologie et Evolution du Vivant (FR3284 CNRS).

bioRxiv preprint first posted online Nov. 5, 2018; doi: http://dx.doi.org/10.1101/461947. The copyright holder for this preprint (which was not peer-reviewed) is the author/funder, who has granted bioRxiv a license to display the preprint in perpetuity.
It is made available under a CC-BY-NC-ND 4.0 International license.

[2]: Address correspondence to maud.tenaillon@inra.fr. The authors responsible for distribution of materials integral to the findings presented in this article in accordance with the policy described in the Instructions for Authors is Christine Dillmann (christine.dillmann@inra.fr).

ABSTRACT. 200 words max

We undertook divergent selection experiments (Saclay DSEs) to investigate the genetic bases of phenotypic evolution in two inbred maize inbred lines, F252 and MBS847. The selected trait was flowering time. After 13 generations of selection, we obtained five distinct populations with a time-lag of roughly two weeks between Early- and Late/VeryLate-flowering populations. We used this unique material to characterize the genome-wide transcriptomic response to selection in the shoot apical meristem before, during and after floral transition in realistic field conditions during two consecutive years. We validated the reliability of performing RNA-sequencing in uncontrolled conditions. We found that roughly half of maize genes were expressed in the SAM, 59.3% of which were differentially expressed. We detected differential expression across meristem status, but also retrieved a subset of 2,451 genes involved in the response to selection. Among these, 22 genes displayed known function in maize flowering time. Furthermore, they were more often shared between inbreds than expected by chance, suggesting convergence of gene expression. We discuss new insights into the expression pattern of key players of the underlying gene regulatory network including *ZCN8*, *RAP2.7*, *ZMM4*, *KN1*, *GA2ox1*.

bioRxiv preprint first posted online Nov. 5, 2018; doi: http://dx.doi.org/10.1101/461947. The copyright holder for this preprint (which was not peer-reviewed) is the author/funder, who has granted bioRxiv a license to display the preprint in perpetuity.
It is made available under a CC-BY-NC-ND 4.0 International license.

INTRODUCTION.

Artificial selection experiments are designed to investigate phenotypic evolution of complex traits and its genetic bases. By combining these experiments and current sequencing tools, a variety of questions can be addressed (Hendry, 2013): What are the limits to the evolution of traits? What are the underlying patterns of allele frequency changes? How many loci are involved in the response to selection and what are their effect size distribution? What is the relative contribution of standing genetic variation versus *de novo* mutations to the response? Do these mutations perturb the level of gene expression or their amino acid sequence? To which extent convergent phenotypic evolution is sustained by the same genetic bases? Because artificial selection experiments are extremely time costly, they have most often been conducted in model organisms with a short generation time, prokaryotes such as *E. coli* (Tenaillon et al., 2012; Good et al., 2017) or, eukaryotes such as yeast (Burke et al., 2014), fruitfly (Burke et al., 2010; Graves et al., 2017), domestic mouse (Chan et al., 2012), *C. elegans* (Teotonio et al., 2017).

Long-lasting evolution experiments are much rarer in vascular plants (but see (Goldringer et al., 2006; Roels and Kelly, 2011; Gervasi and Schiestl, 2017). Maize however stands as an exception: Cyril G. Hopkins started the historical heritage of selection experiments in this model species by launching the Illinois divergent selection for protein and oil content in 1896 (Dudley and Lambert, 1992). Since then, six other experiments have been undertaken: two for increased prolificacy (Maita and Coors, 1996) and grain yield (Lamkey, 1992), two for divergent seed size (Moose et al., 2004) and ear length (Lopez-Reynoso and Hallauer, 1998), and two for divergent flowering time (Durand et al., 2010), called hereafter Saclay's Divergent Selection Experiments (DSEs). One important observation from these experiments is that the response to selection is generally steady over generations (reviewed in

bioRxiv preprint first posted online Nov. 5, 2018; doi: http://dx.doi.org/10.1101/461947. The copyright holder for this preprint (which was not peer-reviewed) is the author/funder, who has granted bioRxiv a license to display the preprint in perpetuity.
It is made available under a CC-BY-NC-ND 4.0 International license.

(Lorant et al., 2018)). This is particularly intriguing for the Saclay's DSEs that started from inbred lines with limited standing variation (<1.9%) and evolved under very small population size. In Saclay's DSEs, divergent selection was applied over 16 generations, and generated considerable phenotypic response with up to three-weeks difference between early and late flowering populations (Durand et al., 2015), a range comparable to what is observed among the maize European Nested Association Mapping panel when evaluated across multiple environments (Lehermeier et al., 2014). The dynamics of the response to selection in Saclay's DSEs is consistent with a continuous input of new mutations (Durand et al., 2010). The use of markers also revealed the contribution of complete sweeps from standing genetic variation (Durand et al., 2015). The combination of both new mutations and standing variation is consistent with the known complexity of flowering time determinism in maize, and a high mutation target, i.e. >100 loci (Buckler et al., 2009).

In plants, flowering is initiated by the transition of the Shoot Apical Meristem (SAM) from a vegetative status where the SAM produces leaves, to a reproductive status where the SAM produces reproductive organs. Because floral transition (FT) induces irreversible developmental changes that ultimately determine flowering time and the completion of seed development in suitable conditions, it is of key adaptive value. FT is tuned by a gene regulatory network (GRN) that integrates environmental and endogenous cues, and translates them to initiate flowering when the time is most favorable. This network is now well described in the model species *Arabidopsis thaliana* with few hundreds of described genes (Bouche et al., 2016), but profound differences with maize have been pointed out. For instance, in contrast to *A. thaliana* maize does not exhibit vernalization response; and some of the major floral maize genes such as *ZMM4* and *ID1* have no homologs in *A. thaliana* (Colasanti et al., 1998).

bioRxiv preprint first posted online Nov. 5, 2018; doi: http://dx.doi.org/10.1101/461947. The copyright holder for this preprint (which was not peer-reviewed) is the author/funder, who has granted bioRxiv a license to display the preprint in perpetuity.
It is made available under a CC-BY-NC-ND 4.0 International license.

In maize, the currently described GRN is still very limited. It encompasses ~30 genes. Among them, *ZCN8* encodes a florigen protein that migrates through the phloem from the leaf to the SAM triggering via its accumulation, the reprogramming of the SAM to FT (Meng et al., 2011). *ZCN8* interacts with the floral activator *DLF1* (Muszynski et al., 2006), and its expression is partially controlled by another activator, *ID1* (Meng et al., 2011). *ZCN8* and *DLF1* act upstream *ZMM4*, a floral meristem identity integrator, which when overexpressed in the SAM leads to early-flowering (Danilevskaya et al., 2008). The transcription factor *RAP2.7* encoded by a gene downstream of the cis-regulatory element *VGT1*, is a negative regulator of flowering time (Salvi et al., 2007) and putatively modulates the expression of *ZMM4* (Dong et al., 2012). Among other genes of the maize flowering pathway, *ZmCCT* is central to photoperiod response (Hung et al., 2012). Mutations at this gene have contributed to the loss of photoperiod response of maize in temperate regions, allowing growth under long-days. Endogenous signals are delivered by the GA signaling pathway, the autonomous pathway, and the aging pathway through the action of miR156/miR172 genes. Interestingly, sucrose levels in sources leaves and carbohydrates export to sink tissues, also appear to play a main role in floral induction. For instance, metabolic signatures in mature leaves associate with the expression of *ID1*, and may contribute to the control of florigens (Coneva et al., 2012).

Here we used early- and late- evolved progenitors from the two Saclay's DSEs (Durand et al., 2010), i.e. two different genetic backgrounds, to (i) characterize the genome-wide transcriptomic response to selection; (ii) identify key players of the underlying GRN; (iii) test for convergence of selection response at the gene level between genetic backgrounds. We evaluated transcriptomic response from RNA-seq of the SAM. SAMs were sampled from plants grown under agronomical field conditions before, during and after floral transition. In addition, we used qRT-PCR to evaluate in multiple organs, the expression of

bioRxiv preprint first posted online Nov. 5, 2018; doi: http://dx.doi.org/10.1101/461947. The copyright holder for this preprint (which was not peer-reviewed) is the author/funder, who has granted bioRxiv a license to display the preprint in perpetuity.
It is made available under a CC-BY-NC-ND 4.0 International license.

three genes of the GRN (*ZMM4*, *ZCN8*, *RAP2.7*), as well as two candidate genes previously detected as associated to flowering time variation in Saclay's DSEs, *UBC-like* and *EiF4A* (Durand et al., 2012).

RESULTS.

We used a unique material created by divergent selection for flowering time starting from two maize inbred lines, the Saclay's DESs, to investigate the determinants of maize floral transition. We chose 5 progenitors from two DSEs after 13 generations of selection: one Early (FE), one Late (FL) and one VeryLate (FVL) from the F252 DSE, and one Early (ME) and one Late (ML) from the MBS DSE (Figure S1). Phenotypic response revealed roughly two weeks differences between Early and VeryLate F252 populations, and Early and Late MBS populations (Figure 1). We used offspring derived by selfing from these progenitors, first to evaluate the timing of FT using meristem observations, and second, to collect samples for expression analyzes. We placed a special emphasize on differentially expressed (DE) genes that may have contributed to the response to divergent selection, and performed for five of them a more detailed expression survey in four organs.

Timing of floral transition.

We collected between 18 and 35 SAMs from progenies of each five progenitors. Plant developmental stages were defined as the number of visible leaves. We defined the SAM Status based on shape and length as Vegetative (V), Transitioning (T) or Reproductive (R) (Figure S2, Table 1). We determined the timing of FT of each progenitor as the earliest stage at which we observed a majority of transitioning SAMs. We made three important observations from the timing of FT (Table 1): (1) FT occurred later in MBS than in F252

bioRxiv preprint first posted online Nov. 5, 2018; doi: http://dx.doi.org/10.1101/461947. The copyright holder for this preprint (which was not peer-reviewed) is the author/funder, who has granted bioRxiv a license to display the preprint in perpetuity.
It is made available under a CC-BY-NC-ND 4.0 International license.

consistently with the flowering time difference between these two inbreds; (2) FT occurred at the same plant developmental stage in Early (FE) and Late (FL) genotypes in F252 (8 visible leaves), but occurred at an earlier plant developmental stage (9 visible leaves) in Early (ME) than in Late (ML) MBS progenitors (10 visible leaves); (3) the Very Late F252 progenitor displayed a delayed timing of FT similar to MBS genotypes, with a year effect – FT occurred at 9 and 10 visible leaves for Year 1 and 2 respectively. Overall, we therefore evidenced a direct link between FT and flowering time, with later occurrence of FT in VeryLate or Late genotypes as compared with Early.

Genome-wide patterns of gene expression as determined by RNA-seq.

We sequenced 25 RNA-Seq libraries (Table 1) and generated between 19,711,727 and 33,475,403 51 bp single-reads per library (Table S1). After trimming, filtering and mapping steps, we recovered between 29.87% and 47.22% of the reads (Table S1) that were used to estimate gene expression. We computed expression of annotated genes in the maize reference genome v3 by relying on the corresponding number of raw counts obtained from the longest transcript of each of 39,066 genes (Table S2). After filtering and normalization, we recovered a subset of 21,488 genes (55%) for which there was at least one count per million reads in half of our libraries. We verified that the libraries considered as Replicates (same Progenitor, same SAM Status) did cluster together (Figure 2), and that differences among Progenitor/Status were higher than differences among replicates (data not shown). The distributions of the normalized counts indicated lowest and highest quartiles comprised between ~30 and ~500, with a median depth around 200 (Figure S3).

We computed pairwise correlations of normalized counts across all 25 libraries. Pearson's correlation coefficients ranged between 0.83 (ME_T_2 vs FE_V_1) and 0.99 (FE_T_2 vs FL_T_2). These elevated values indicate that patterns of gene expression are

bioRxiv preprint first posted online Nov. 5, 2018; doi: http://dx.doi.org/10.1101/461947. The copyright holder for this preprint (which was not peer-reviewed) is the author/funder, who has granted bioRxiv a license to display the preprint in perpetuity.
It is made available under a CC-BY-NC-ND 4.0 International license.

overall well conserved across libraries. In addition, multidimensional scaling revealed a separation between lines on the axis 1, and among SAM Status on the axis 2 for F252 (Figure 2). Altogether, our methodology revealed repeatable patterns and a visible signal of differential gene expression.

DE genes and targets of selection.

We performed 27 contrasts to detect DE genes (Table 2). In total, we detected 12,754 DE genes, 49% of which were significant in more than one contrast (Table S3). We sorted the contrasts into different categories (Table 2 & Table S3). The Year and the Line categories combined DE genes exhibiting differential expression between years or lines (F252 *versus* MBS), respectively. The Status category combined DE genes whose expression varied between two SAM status either in the F252 ([StatusF]) or MBS ([StatusM]) genetic backgrounds. The Selection category combined DE genes exhibiting differential expression between early (FE) and late (FL or FVL) progenitors for the F252 DSE ([selF]), or between early (ME) and late (ML) progenitors for the MBS DSE ([selM]. The Status x Progenitor interactions category combined DE genes displaying differential expression between two SAM status in one but not all progenitors from the same line ([StatusProg]). Within this last category, we considered as selected within the F252 line ([SelF][StatusProg]), the subset of DE genes displaying differential expression between SAM status for FE but not for the corresponding SAM status for either FL or FVL, and reciprocally. Note that for MBS, no DE gene could be found in the corresponding [SelM][StatusProg] category because we detected no DE genes between ME_T and ME_R (Table 2).

Out of the 12,754 DE genes, 3,713 displayed a Year effect, 8,228 a Line effect, 6,568 displayed a Status effect, and 2,499 a Status x Progenitor interactions effect (Table 2). We detected 4,682 and 2,719 DE genes with a Status effect in F252 and MBS, respectively

bioRxiv preprint first posted online Nov. 5, 2018; doi: http://dx.doi.org/10.1101/461947. The copyright holder for this preprint (which was not peer-reviewed) is the author/funder, who has granted bioRxiv a license to display the preprint in perpetuity.
It is made available under a CC-BY-NC-ND 4.0 International license.

(Table 2). For MBS, we found 446 DE genes within the Selection category. For F252, we found 2,120 in the Selection category, that comprised 748 DE genes between Early and Late or Very Late F252 progenitors ([SelF]). Considering both F252 and MBS, there were 2,451 DE genes falling into the Selection category (Table 2 & Table S4).

From the normalised counts, we determined for each DE gene its average expression per Progenitor per Status, corrected for the Year effect using a linear model. We further normalised average gene expression by the overall mean, so that a negative value corresponds to under-expression, and a positive value to over-expression. We discarded from the rest of the analyses 1,481 DE genes that displayed a Year effect only, 3,262 that displayed a Line effect only as well as 641 DE genes displaying a combined Year and Line effect (Table S3 & S4). The majority (77%) of the 7,370 remaining DE genes were significant in more than one contrast.

We performed a principal component analysis on the set of 7,370 DE genes, and attributed each one of them to a principal component axis based on correlation coefficient values (Table S4). We plotted heat maps of the 4 first components which explained respectively, 38%, 27%, 9%, 7% of the variance in gene expression. The first PCA component (3,850 DE genes) corresponded to DE genes that differentiated lines, and SAM status in F252 (Figure 3A, Table 3). The second PCA component (2,388 DE genes) was enriched for DE genes associated with SAM status in F252 and in ME (Figure 3B, Table 3). The third PCA component encompassed 522 DE genes whose expression was specific to FVL progenitor as opposed to FE and FL, and varied across status in FE, FL and ME (Figure 3C, Table 3). The fourth component regrouped 278 DE genes whose expression was modified during floral transition (Figure 3D, Table 3). Altogether the first four components regrouped >95% of the set of 7,370 DE genes which represented 55.2% of all DE genes (Table 3).

bioRxiv preprint first posted online Nov. 5, 2018; doi: http://dx.doi.org/10.1101/461947. The copyright holder for this preprint (which was not peer-reviewed) is the author/funder, who has granted bioRxiv a license to display the preprint in perpetuity.
It is made available under a CC-BY-NC-ND 4.0 International license.

Out of 2,451 DE genes of the Selection category, the PC1 exhibited the greatest proportion of all PCs (46.3%, Table 3) followed by PC2 (30.1%, Table 3). We investigated the relative contribution of genes differentially expressed between FE and FL, FE and FVL, ME and ML to the Selection category. As expected from the phenotypic response – larger between FE and FVL than between FE and FL (Figure 1) – a greater proportion of DE genes were found between FE and FVL (576) than between FE and FL (346). Comparisons of ME and ML revealed 446 DE genes (Figure S4). For F252, we found that a majority of DE genes of the Selection category were detected within the Status x Progenitor interactions category (Figure S4).

To test for evidence of convergence in the response to selection between lines MBS and F252, we asked whether the count of shared DE genes belonging to the Selection category in F252 and MBS (Table S4) was significantly different from a null expectation. There were 115 shared DE genes when including Selection within Status x Progenitor interactions (for F252), and 64 shared DE genes when excluding them. This was significantly more than expected as tested with a two-sided exact Poisson test (with 115: expected=74 and P-value= $9.1\ 10^{-06}$, with 64: expected=26 and P-value= $3.8\ 10^{-10}$).

Altogether, our data revealed interesting features: (1) 59.3% of the 21,488 expressed genes were differentially expressed; (2) DE genes were most abundant in the Line (8,228), followed by Status (6,568) and Year (3,713) categories; (3) MBS displayed less genes of the Selection category than F252; (4) There was an excess of shared DE genes in the Selection category between lines.

Functional relevance of DE genes.

In order to get more insights into the functions of detected DE genes, we undertook several approaches. First, we established from the literature a complete list of flowering time

bioRxiv preprint first posted online Nov. 5, 2018; doi: http://dx.doi.org/10.1101/461947. The copyright holder for this preprint (which was not peer-reviewed) is the author/funder, who has granted bioRxiv a license to display the preprint in perpetuity.
It is made available under a CC-BY-NC-ND 4.0 International license.

genes whose function has been at least partially validated at the molecular level (Table S5 and references herein). Note that 39 of them are already connected in the maize flowering GRN (Figure S5), and only one (GRMZM2G022489, CG1) did not have raw counts information from our RNA-Seq dataset. We referred to this list of 70 genes as FT_candidates. Second, we relied on the results of the most recent GWA study on maize male and female flowering time (Navarro et al., 2017) to establish a list of 984 GWA_candidates (1001 genes were extracted from (Navarro et al., 2017), 984 of which presented raw counts information from our RNA-Seq dataset, Table S5). Third, we tested for enrichment/depletion of our DE genes in Mapman and Kegg functional categories (Table S6).

Out of 70 and 984 of the FT_candidates and GWA_candidates, 54 and 294 respectively displayed differential gene expression (Table 3). Comparatively, FT_candidates therefore presented a greater enrichment of DE genes than GWA_candidates (77.1% versus 29.9%, Table 3). After discarding the DE genes displaying either a significant Year or Line effect only, or a combination of both, there were 38 and 185 DE genes left for FT_candidates and GWA_candidates respectively. Nearly all of the 38 FT_candidates displayed differences between Status in F252 (33) and to a lesser extent in MBS (18). Remarkably, 22 of them also belonged to the Selection category in F252 (Table S5) including 6 genes connected in the maize FT GRN: *KN1*, *ELF4*, *DLF1*, *GIGZ1A*, *GIGZ1B*, *PHYA1* (Figure S5). Likewise, for GWA-candidates, we found a majority of the remaining genes with differences between Status in F252 (119), and to a lesser extent in MBS (58) and the Selection category included 77 genes for F252, 10 genes for MBS, and two genes for both (Table S5). Comparatively, the proportion of genes falling into the Selection category among FT_candidates (22/70=31.4%) was therefore much higher than among GWA_candidates (79/984=8.0%).

We asked what was the proportion of DE genes that were correlated to the first four PC axes, (i) among all DE genes, (ii) among DE genes belonging to the Selection category,

bioRxiv preprint first posted online Nov. 5, 2018; doi: http://dx.doi.org/10.1101/461947. The copyright holder for this preprint (which was not peer-reviewed) is the author/funder, who has granted bioRxiv a license to display the preprint in perpetuity.
It is made available under a CC-BY-NC-ND 4.0 International license.

(iii) among FT_ or GWA_candidates. Our results revealed a clear enrichment of PC1 for the Selection category and candidates (>46.3% while only 30.2% of DE genes belonged to PC1), and of PC2 for the Selection category (30.1%, Table 3). Functional categories enrichment and depletion analyzes revealed specific patterns for each four PC axes (Table S6).

In summary, we showed that both FT_ and GWA_candidates are enriched for Status-related DE genes; and we found that a large proportion of FT_candidates is related to the differential response to selection.

Expression of 5 genes as determined by qRT-PCR and correlation with RNA-Seq measures.

We examined the expression of five genes, including three key genes of the maize flowering GRN and two candidate genes using qRT-PCR (Figure S5). We focused on four organs: the immature part, mature part and the sheath of the last visible leaf, and the SAM. We measured gene expression by the amplification Cycle threshold (C_T). We used *ZmGRP1* as a reference gene to normalize cDNA quantities. We performed three biological replicates but only two of them were used for *Eif4A*. We also incorporated with the amplification of each gene control samples for F252 and MBS for which all organs were pooled.

Regarding *ZmGRP1* expression in control samples (Table S7), after checking for variance and residues independence we found a significant Line (F= 242.8627, P-value= 1.249e-15) and Year effect (F= 18.3751, P-value= 0.0001828) with significant interaction (F= 191.5834, P-value= 2.621e-14) but no Plate effect (F= 0.3955, P-value= 0.5343464). For the five genes of interest, the Plate effect was confounded with Gene effect (each gene being amplified in a different plate). That we did not observe a Plate effect for control samples amplified with *ZmGRP1* indicated that comparisons among our five genes were accurate.

bioRxiv preprint first posted online Nov. 5, 2018; doi: http://dx.doi.org/10.1101/461947. The copyright holder for this preprint (which was not peer-reviewed) is the author/funder, who has granted bioRxiv a license to display the preprint in perpetuity.
It is made available under a CC-BY-NC-ND 4.0 International license.

We next analysed *ZmGRP1* expression across all samples (Table S8). *ZmGRP1* C_T varied significantly between Lines, Years, Organs, Status:Organs (P-values<0.0428944), thereby indicating substantial variation in the amount of cDNA quantities across samples. We therefore normalized expression of all genes in all organs using *ZmGRP1* (corresponding ratio values (R) are provided Table S8).

Finally, we assessed significant effects across samples for each of the five genes. Overall most effects (Replicate, Progenitor, Status, Organ) were significant, except for the Progenitor and the Status effects in *ZNC8* and *EiF4A* respectively (Table S9).

Patterns of normalized gene expression among replicates can be summarized as follows. The expression of *ZMM4* increased at the time of FT (with significant differences between vegetative and transition status) irrespective of the Organ, Progenitor and Line, and its expression was higher in the SAM than in all other organs (Figures 4A&F). The expression of *ZCN8* exhibited a trend towards increased expression through time in all Organs and all Progenitors. This trend was more pronounced in the SAM with significant increase in expression between the transition and reproductive status in F252 and MBS (Figures 4B&G). *RAP2.7* displayed a significant reduction in the SAM at FT followed by a significant increase in expression at the reproductive stage. This pattern was observed in all Progenitors (Figures 4C&H) but *RAP2.7* displayed an overall lower level of expression in FVL compared with FE and FL (Figure 4C). *RAP2.7* was also more expressed in mature leaves than in any other organs. For *UBC-like*, we observed noticeable differences in the level of expression between FE, and FL and FVL within F252 (Figure 4D). In MBS both alleles were expressed at a similar level than FE in F252 (Figure 4I). We observed no particular timing trend for *EiF4A*, whose expression was fairly stable through time (Figure 4E&J; Table S9).

bioRxiv preprint first posted online Nov. 5, 2018; doi: http://dx.doi.org/10.1101/461947. The copyright holder for this preprint (which was not peer-reviewed) is the author/funder, who has granted bioRxiv a license to display the preprint in perpetuity.
It is made available under a CC-BY-NC-ND 4.0 International license.

In conclusion, qRT-PCR revealed patterns of expression consistent with *ZMM4* and *ZCN8* being floral inducers. Expression of of *RAP2.7* on the other hand was repressed during FT. Interestingly, we noticed differences in expression between Early and Late or VeryLate Progenitors in F252 for *UBC-like* and to a lesser extent for *RAP2.7*.

We tested the correlation between expression from qRT-PCR (measured by R) and by the normalized counts from RNA-Seq. While we were able to detect *ZCN8* expression in the SAM via qRT-PCR (Figure 5B), the RNA-Seq analysis did not reveal evidence of expression of *ZCN8*. Because *ZCN8* belongs to a multigenic family, it is possible that the filtering steps did not allow for proper evaluation of its expression using RNA-seq.

Among the 4 remaining genes, *ZMM4*, *RAP2.7* and *UBC-like* displayed a significant positive correlation coefficient (Figure S6). *ZMM4* exhibited the highest value of all three (r=0.82, P-value=0.004). The pattern of *EiF4A* with no correlation detected, remained difficult to interpret.

DISCUSSION

Saclay's DSEs have revealed remarkable shifts at the phenotypic level, with the production, in only 13 generations of divergent selection, of populations that flower two weeks apart in the two genetic backgrounds F252 and MBS respectively (Figure 1). Here, we showed that the timing of FT is intimately linked to flowering time, with earlier transition in early progenitors as compared with late progenitors. We used evolved lines at generation 13 to examine the transcriptomic response to divergent selection, refine the underlying GRN, and test whether the observed phenotypic convergence is sustained by convergence at the transcriptomic level. We generated RNA-seq from pooled samples of SAM before/during/after FT. All samples were collected in the field during two consecutive years.

bioRxiv preprint first posted online Nov. 5, 2018; doi: http://dx.doi.org/10.1101/461947. The copyright holder for this preprint (which was not peer-reviewed) is the author/funder, who has granted bioRxiv a license to display the preprint in perpetuity. It is made available under a CC-BY-NC-ND 4.0 International license.

We recovered expression for 55% of all annotated maize genes indicating that about half of them were expressed in the SAM. We detected differential expression for roughly 59% of them.

Expression varies primarily across developmental stages.

As expected, expression varied more between lines than among developmental stages, with a proportion of DE genes exhibiting a Line or a Status effect of 64% and 51% respectively (Table 2). That variation among Status concern a large proportion of genes conformed previous report (Swanson-Wagner et al., 2012), and indicates that Status is a key component of gene expression rewiring, particularly for F252 (Figures 2 & 3). For MBS, the pattern was not as strong in part because we lacked the vegetative Status for one of the late Progenitor (ML, Table 1). For the early (ME), however, the Status response was visible in heatmaps of the genes most correlated with PC2, 3 and 4 (Figure 3).

Given the complexity of the underlying network and its regulation, we expect the expression of few genes to affect in turn the expression of a myriad of response genes detected in our analyzes; and functional categories of these response genes are likely extremely broad given the variety of processes at work. The timing of FT is regulated by transcriptional and post-translational regulatory mechanisms, including DNA methylation, chromatin modification, small and long noncoding RNA activity (Andres and Coupland, 2012). For example, chromatin modifications in *ID1* modulate the expression of *ZCN8* in temperate maize (Mascheretti et al., 2015). Signaling from leaf to the SAM includes transmission of florigens (such as *ZCN8*) produced in the leaf and transported through the phloem sieve elements, making interactions with protein membranes as well as protein-protein interactions important determinants of FT. Finally, upregulation of protein targeting, amino acid and DNA synthesis, as well as an increase ATP production has been observed

bioRxiv preprint first posted online Nov. 5, 2018; doi: http://dx.doi.org/10.1101/461947. The copyright holder for this preprint (which was not peer-reviewed) is the author/funder, who has granted bioRxiv a license to display the preprint in perpetuity.
It is made available under a CC-BY-NC-ND 4.0 International license.

during the floral transition stage in the SAM (Takacs et al., 2012). As expected, we found among DE genes significant enrichment in many functional categories including amino acid metabolism, ATP synthesis, DNA, RNA, signaling, interactions, transport (Table S6).

While response to endogenous signals by means of the autonomous pathway (Figure S5) occupies a central role in floral transition in maize temperate lines (Colasanti and Coneva, 2009), environmental signals are likely important too. We indeed found enrichment for the environmental adaptation functional category, among our DE genes, (Table S6). One of the main steps of maize temperate adaptation has been the rapid loss of photoperiod (Hung et al., 2012; Teixeira et al., 2015). Besides photoperiod, thermoregulation of flowering through the accumulation of degree days and threshold effects is also well-recognized in temperate maize and generates interannual variation in flowering time (Teixeira et al., 2015). Surprisingly, however, this interannual environmental variation impacted less patterns of gene expression than developmental stages or genetic backgrounds (29% only of all DE genes exhibited a Year effect). This important observation first indicates that RNA-seq experiments can be reliably interpreted in realistic field conditions. Second, it is consistent with the idea that selection during the breeding process has favored stability of expression across environments to ensure a reliable developmental outcome independently of environmental variation. Such robustness to perturbation, also called phenotypic canalization, is likely to evolve when constant phenotypic optimum (inbred line phenotype) is selected for (Abley et al., 2016). Hence, genomic regions selected during modern breeding in temperate inbreds exhibit reduced genotype x environment interactions for grain yield, thereby limiting their plastic response (Gage et al., 2017).

bioRxiv preprint first posted online Nov. 5, 2018; doi: http://dx.doi.org/10.1101/461947. The copyright holder for this preprint (which was not peer-reviewed) is the author/funder, who has granted bioRxiv a license to display the preprint in perpetuity.
It is made available under a CC-BY-NC-ND 4.0 International license.

Number of selected DE genes correlates with phenotypic response.

Given our material, we paid a special attention to DE genes involved in the response to divergent selection for flowering time. Altogether they represent 19% of all DE genes. These included genes that were differentially expressed between Progenitors within Line, as well as DE genes between Early, and Late or Very Late Progenitors within Status x Progenitor interactions for F252. Interestingly, most DE genes of the Selection category in F252 were detected from Status x Progenitor interactions (Figure 3). Consistently we found enrichment of DE genes from the Selection category across all PCs, but more so for PC1 and PC2 (Table 3).

Overall, F252 displayed more DE genes within the Selection category than MBS (2120 vs 446). This is in line with overall lower level of residual heterozygosity detected in the former (Durand et al., 2015). However, if we considered only the Early and Late progenitors of each Line (discarding the VeryLate Progenitor of F252), we obtained the inverse trend, with less DE genes for F252 (346) than for MBS (446) (Table 2, Figure S4). This pattern was consistent with a lack of phenotypic response in the Late F252 population after 7 generations of selection but a continuation in the Late MBS population until G13 (Durand et al., 2015). Such lack may be explained by the strong selection operated in the VeryLate F252 population that in turn relaxed selection in the Late F252 population (Figure 1).

Linkage disequilibrium is expected to be pervasive in our small populations, perpetuated by selfing. One could therefore argue that genes of the Selection category are mainly driven by fixation of large chromosomal regions during the first generations of selection, generating where allelic variation exists, blocks of alleles differentially expressed between Early and Late progenitors. We further tested the clustering of genes by fitting a generalized linear model where the counts of DE genes of the Selection category were

bioRxiv preprint first posted online Nov. 5, 2018; doi: http://dx.doi.org/10.1101/461947. The copyright holder for this preprint (which was not peer-reviewed) is the author/funder, who has granted bioRxiv a license to display the preprint in perpetuity.
It is made available under a CC-BY-NC-ND 4.0 International license.

determined by the number of maize genes in 1Mb non-overlapping windows and a quasiPoisson distributed error. We found an overall significant overdispersion (dispersion parameter=1.17, P-value=1.04 10^{-7}), albeit with noticeable differences among chromosomes (P-value=0.0006). Chromosomes 1, 6 and 10 were significantly enriched for DE genes of the Selection category, while chromosomes 4, 7, 9 were significantly depleted.

At a first glance, these results are consistent with random fixation of segregating alleles by genetic hitchhiking accompanying the sweep to fixation of a single beneficial mutation. However, several lines of arguments support that DE genes of the Selection category do contribute to the observed phenotypic response to selection. First, the majority of these genes (91.1%) belonged to the 4 first PCs and therefore exhibited patterns consistent with Status changes. Second, many genes selected in F252 displayed Status x Progenitor interactions (Figure 3). Third, these genes were depleted for "unknown" function or "not assigned" to a function (Table S6); this is consistent with an enrichment for flowering time genes that are likely well annotated. Finally, genes of the Selection category encompassed 22 out of 54 FT_candidates that were differentially expressed, a proportion of 40.7 % that far exceeded the proportion of genes of the Selection category among all DE genes (19.2%).

Selected DE genes are enriched for genes of the flowering time network.

Among FT_candidates involved in the response to selection (Table S5), six were already connected in the GRN (Figure S5). They belong to a variety of pathways: *PHYA1* is a photoreceptor (Sheehan et al., 2004), *KN1* belongs to the GA pathway (Bolduc and Hake, 2009), *ELF4* is involved in the photoperiod pathway (Yang et al., 2013), while *GIGZ1A*, *GIGZ1B* connect the latter to the circadian clock pathway (Miller et al., 2008), and *DLF1* is a floral activator (Muszynski et al., 2006). Flowering time is positively correlated with gibberellin accumulation in maize (Thornsberry et al., 2001). Previous results suggest that

bioRxiv preprint first posted online Nov. 5, 2018; doi: http://dx.doi.org/10.1101/461947. The copyright holder for this preprint (which was not peer-reviewed) is the author/funder, who has granted bioRxiv a license to display the preprint in perpetuity.
It is made available under a CC-BY-NC-ND 4.0 International license.

KN1 displays a complex pattern of expression that differs among tissues, and that it contributes to decrease gibberellin accumulation through upregulation of *GA2ox1* (Bolduc and Hake, 2009). Here we found a pattern of upregulation of *KN1* expression in all progenitors during and after FT (Figure 5A). Moreover, the expression of *GA2ox1* is downregulated during FT in all progenitors (Figure 5B) mirroring the pattern observed in rice (Sakamoto et al., 2001). Promotion of FT necessitates a critical level of *DFL1* mRNA abundance, and its expression is subsequently downregulated after FT (Muszynski et al., 2006). Interestingly we found a greater level of mRNA abundance before FT in VeryLate progenitor compared with the other progenitors, suggesting that the former has evolved a distinct threshold level above which FT is initiated.

Among the two candidate genes previously detected as associated to flowering time variation in our selection experiment settings, *EiF4A* was detected in the Selection category for the F252 line (Durand et al., 2010). This gene also displayed significant contrast across status within F252 (Table S5). Intriguingly, qRT-PCR revealed significant differences in expression neither across status nor progenitors for *EiF4A* (Figure 4). Instead there were significant differences in expression between Early and Late or VeryLate progenitors in F252 for *UBC-like*, the second candidate gene located in the vicinity of *EiF4A* (Durand et al., 2012). However, *UBC-like* did not display significant contrasts across status and progenitors in the RNA-seq analysis (Table S5). Hence, while we found in general good agreement between the two methods for three out of four genes with significant correlations (Figure S6), our results suggest that the two methods are complementary rather than redundant. This may have several origins: the sensibility of the methods likely differs, and we considered a single transcript per gene for RNA-seq analyzes.

The overall observed patterns were consistent with the roles of *ZMM4* and *ZCN8* in promoting floral transition in temperate maize, with upregulation of *ZMM4* in all organs at

bioRxiv preprint first posted online Nov. 5, 2018; doi: http://dx.doi.org/10.1101/461947. The copyright holder for this preprint (which was not peer-reviewed) is the author/funder, who has granted bioRxiv a license to display the preprint in perpetuity.
It is made available under a CC-BY-NC-ND 4.0 International license.

FT – including the SAM – in both F252 and MBS (Danilevskaya et al., 2008) (Figure 4A&F), and increased expression of *ZCN8* during FT (Meng et al., 2011) in the SAM also in both inbred lines (Figure 4B&G). In addition, we report here the first qRT-PCR survey of the expression of *RAP2.7* in the SAM during FT (Figure 4C&H). It displayed patterns consistent with its role as a negative regulator of flowering time (Salvi et al., 2007). Interestingly, we also revealed the role of *RAP2.7* in the response to selection. Previous studies have shown that the presence of miniature transposon in a conserved non-coding sequence upstream *RAP2.7* is associated with early-flowering (Salvi et al., 2007; Ducrocq et al., 2008). More recently a model has been proposed whereby methylation spreading from the transposon reduces the expression of the *RAP2.7* in the leaves causing early flowering (Castelletti et al., 2014). In contrast, we found that low expression in the SAM correlates with late-flowering. Because the MITE insertion is present in F252 (Ducrocq et al., 2008) and unlikely polymorphic among our samples, differential expression among alleles may be caused by a complex regulation including the action of miR172 (Figure S5).

Besides those FT_candidates already connected in the GRN, others merit attention. For instance, we detected the three *RAMOSA* genes (Table S5) that act together to determine inflorescence branching (Vollbrecht et al., 2005; Bortiri et al., 2006), one of which, *RA1*, may be in part regulated by sugar signaling (Satoh-Nagasawa et al., 2006). In addition, we confirmed the suspected role of *ZMM26* (GRZM2G046885) in maize flowering time transition (Alter et al., 2016) as it was found under selection in F252 (Table S5). The more pronounced downregulation of *ZMM26* at the time of FT may be involved in delayed flowering in the VeryLate progenitor (Figure 5C). Finally PIF3.1, a member of a family of phytochrome interacting factor in maize that mediates plant response to various environmental factors (Kumar et al., 2016), was found under selection in F252. The trend

bioRxiv preprint first posted online Nov. 5, 2018; doi: http://dx.doi.org/10.1101/461947. The copyright holder for this preprint (which was not peer-reviewed) is the author/funder, who has granted bioRxiv a license to display the preprint in perpetuity.
It is made available under a CC-BY-NC-ND 4.0 International license.

towards increased expression in the SAM at FT in the Early progenitors of both inbreds indicates a potential role in promoting early flowering (Figure 5E&F).

Genetic convergence between inbred lines is detected.

We detected convergence of transcriptome response between lines submitted to the same selection pressure, which translated into an excess of shared DE genes of the Selection category between lines. Such convergence of molecular phenotypes may result from distinct regulatory mechanisms of gene expression: selection of mutations in trans-acting factors that modulate expression of entire pathways (Li et al., 2013); or selection of mutations in cis-acting factors. With the former, we do not necessarily expect expression convergence to translate into genetic convergence at the locus level, as different factors targeting the same sets of genes may be selected for in different populations. Conversely, with cis-acting factors, genetic convergence at the locus level is more likely to be detected. An example of this situation was recently illustrated by the selection of two independent cis-regulatory variants at the flowering time gene *ZCN8* during early domestication and later diffusion of maize (Guo et al., 2018).

Interestingly, these two variants pre-existed before the onset of selection in teosinte populations. Likewise, in our DSEs, we found an example of selection in a genomic region encompassing several genes among which *EiF4A*, which displayed residual heterozygosity in the initial F252 seed lot. This region subsequently underwent differential fixation of the two alleles in the Early and VeryLate F252 progenitors (Durand et al., 2012). The reasons for the maintenance of such extended regions of residual heterozygosity after multiple generations of selfing used to create inbred lines, are still unclear. Selection against inbreeding depression may act to maintain residual heterozygosity. In maize, however, this type of selection most often creates stretches of heterozygosity that are unique or shared by very few lines

bioRxiv preprint first posted online Nov. 5, 2018; doi: http://dx.doi.org/10.1101/461947. The copyright holder for this preprint (which was not peer-reviewed) is the author/funder, who has granted bioRxiv a license to display the preprint in perpetuity.
It is made available under a CC-BY-NC-ND 4.0 International license.

(Brandenburg et al., 2017). It is therefore unlikely that it would create patterns of convergence, unless trans-acting factors are involved.

Finally, convergence of gene expression between our populations may originate from *de novo* mutations acquired independently across lineages. Examples of such convergence exist *in natura* such as the well-known case of pelvic reduction in freshwater stickleback (Chan et al., 2010). In experimental evolution systems such as bacteria, parallel *de novo* mutations have been often observed at the gene and even nucleotide level during adaptation to antibiotic dosage (Laehnemann et al., 2014), to nutrient availability and growth conditions (Turner et al., in press), and during acclimation to high temperature (Tenaillon et al., 2012). In this last example, first-step mutations in the evolved lines have been observed at a single gene in multiple replicates. These mutations restore the ancestral physiological state and growth efficiency at high temperature. They occur in a trans-acting factor modulating the expression of hundreds of downstream genes (Rodriguez-Verdugo et al., 2016). Such pattern is consistent with our observations with convergence of expression at both candidate and response genes.

CONCLUSION.

We used two divergent selection experiments with controlled genetic backgrounds and little residual heterozygosity to characterize the genome-wide transcriptomic response to selection for flowering time. Throughout this study, we have demonstrated the reliability of performing RNA-seq experiments in realistic field conditions. We have shown that the meristem developmental status is the main source of differential gene expression. We uncovered a subset of genes involved in the response to selection. This subset of genes likely encompasses a majority of response genes; but also displays a strong enrichment for flowering time genes with evidence of convergence of expression between lines sustaining

bioRxiv preprint first posted online Nov. 5, 2018; doi: http://dx.doi.org/10.1101/461947. The copyright holder for this preprint (which was not peer-reviewed) is the author/funder, who has granted bioRxiv a license to display the preprint in perpetuity.
It is made available under a CC-BY-NC-ND 4.0 International license.

phenotypic divergence. Modeling of the floral transition gene network would help dissociating causal from response genes.

MATERIAL AND METHODS.

Plant Material.

We have conducted two independent Divergent Selection Experiments (Saclay DSEs) for flowering time from two commercial maize inbred lines, F252 and MBS847 (MBS). Within each DSE, plants selected as early- or late-flowering were selfed at each generation, and offspring used for the next generation of selection. As a result, we derived from each DSE, two populations of Early- and Late-flowering genotypes previously identified as Early F252, Late F252, Early MBS, Late MBS (Durand et al., 2015), as well as a VeryLate F252 populations. Seeds from selected genotypes at all generations were stored in cold chamber. We traced back the F252 and MBS pedigrees from generation 16 (G16) to the start of the DSEs (G0) (Durand et al., 2015). From pedigrees and flowering time data, we defined 10 families, named respectively FE1, FE2, FL1, FL2.1, FL2.2 for Early and Late F252, and ME1, ME2, ML1, ML2 and ML3 for Early and Late MBS (Figure S1). Note that FL1 corresponds to a Very Late family whose selection was abandoned at G14 for practical reasons – it flowered so late that it was not able to produce viable seeds after G14.

In order to investigate genome-wide changes of gene expression before, during, after flowering transition and contrast those changes between Early and Late genotypes, we sampled progenitors selected at G13 from the two DSEs. Our sampling (Figure S1) encompassed one progenitor from each of the FE1, FL1, FL2-1, ME2, ML1 families. These represent the Early (FE1), Late (FL2-1) and Very Late (FL1) F252 populations (hereafter FE,

bioRxiv preprint first posted online Nov. 5, 2018; doi: http://dx.doi.org/10.1101/461947. The copyright holder for this preprint (which was not peer-reviewed) is the author/funder, who has granted bioRxiv a license to display the preprint in perpetuity.
It is made available under a CC-BY-NC-ND 4.0 International license.

FL, FVL) and the Early (ME2) and Late (ML1) MBS populations (hereafter ME, ML) (Figure S1).

All 5 progenitors were selfed to produce seeds. The resulting progenies were grown in the field at Gif-sur-Yvette France during summer 2012 and 2013. We added as controls, plants from F252 and MBS initial seed lots. We defined developmental stages as the number (n) of visible leaves — the cotyledon leaf being considered as the first one, and named them accordingly Leafn. Based on preliminary observations, we defined 4 to 5 developmental stages per progenitor (FE, FL, FVL, ME, ML) from leaf6 to leaf12 that encompassed the flowering transition (Table 1). Between June 08th and july 9th for 2012 (Year 1) and june 14th and july 19th for 2013 (Year 2), we dissected 4 organs from fresh material on a daily basis: the Shoot Apical Meristem (SAM), the immature and mature part of the last visible leaf (IL, ML), the sheath at the basis of the last visible leaf (S). We recorded the developmental stage of each plant (number of visible leaves) as well as the SAM status: Vegetative (V), Transitioning (T) or Reproductive (R). We established SAM status based on its shape following (Irish and Nelson, 1991) and length. Typical range of lengths are V: 0.1-0.2 mm, T: 0.2-0.35 mm, R>0.35 mm.

For a given organ, we pooled together from 16 to 31 plants from the same progenitor at the same developmental stage (Table 1). We used as controls, plants from the original seed lots for F252 and MBS. These controls were dissected only at stage leaf9 and leaf11 respectively, and all 4 organs were pooled together within a tube. All collected organs were frozen in liquid nitrogen upon collection and stored at -80°C. In total, we gathered 5 progenitors x 4 organs x 4 stages that are 80 samples per year in addition to the F252 and MBS controls. In 2013, we included one more stage for the ML progenitor for a total of 86 samples including the two controls. We performed a single biological replicate in 2012 (Replicate 1) and two biological replicates in 2013 (Replicates 2 and 3) for all organs, except

bioRxiv preprint first posted online Nov. 5, 2018; doi: http://dx.doi.org/10.1101/461947. The copyright holder for this preprint (which was not peer-reviewed) is the author/funder, who has granted bioRxiv a license to display the preprint in perpetuity.
It is made available under a CC-BY-NC-ND 4.0 International license.

the SAM for which a single biological replicate was done each year. Total RNAs of pooled samples were extracted using Qiagen RNeasy Plant kit for SAMs, and using TRIzol reagent (Invitrogen) and ethanol precipitation for other organs. Total RNA was treated with DNAse (Ambion) following the manufacturer's instructions. We evaluated RNA yields using Nanodrop 2000 (Thermo Scientific)

qRT-PCR assays and statistical procedure.

For all samples, 4 µg or less (for samples with <4 µg) of total RNA was reverse transcribed using random hexamers (Thermo scientific), 200 units of Revertaid Reverse Transcriptase (Thermo Scientific), and 20 units of recombinant Rnasin RNase inhibitor (Promega) in a final volume of 20 µl. Simultaneously, all samples were subjected to the same reaction without the RT to verify that there was no genomic DNA contamination. We designed copy-specific primers to amplify the following 5 genes: *MADS-transcription factor 4* (*ZMM4*, GRMZM2G032339), *phosphatidylethanolamine-binding protein8* (*ZCN8*, GRMZM2G179264), *Apetala-2 domain transcription factor* (*RAP2.7*, GRMZM2G700665), *NEDD8-conjugating enzyme Ubc12-like* (*UBC-like*, GRMZM2G102421, *eukaryotic initiation factor4a* (*EiF4A*, GRMZM2G027995). Primer sequences are the following: *ZMM4* F : 5'GGAGAGGGAGAAGGCGGCG 3', R : 5' CTACTCAAGAAGGCGCACGA 3', *ZCN8* F : 5'ATGCGCCACAACTTCAACTG 3', R : 5'GAAGAGTAGAAACCATAGGCCACTGA 3'*RAP2.7* F : 5'CGCCGACATCAACTTCAACC 3', R : 5'CTCCAGGTACAGAGGCGTCA 3', *UBC-like* F : 5'GCTGAGCCGTCACTAAATTGG 3', R : 5'TCCTAGGCACTGAATTGACCC 3', *EiF4A* F : 5' CTGCCAATGTTGCTGACCTT 3', R : 5'CGAAATACCGTGGGAGAGGG 3'. We used *Glycine-rich protein1* (*ZmGPR1=GRMZM2G080603)* with the following primers F:5'-CACAACGCCTTCAGCACCTA-3', R:5'- AAGGTGACGAAGCCGAAGC-

bioRxiv preprint first posted online Nov. 5, 2018; doi: http://dx.doi.org/10.1101/461947. The copyright holder for this preprint (which was not peer-reviewed) is the author/funder, who has granted bioRxiv a license to display the preprint in perpetuity. It is made available under a CC-BY-NC-ND 4.0 International license.

3') as a reference gene with ubiquitous expression among stages and organs following Virvoulet et al. (2011). *ZmGRP1* has been shown to be the second most stably expressed genes among 60 distinct tissues representing different organs x stages (Sekhon et al., 2011).

We used standard qRT-PCR protocols with the SYBR Green PCR Master Mix (Applied biosystems) and the 7500 Real Time PCR System (Applied Biosystems) to evaluate gene expression. We undertook calibration procedure to ensure equivalent PCR efficiency across genes using serial 7-fold dilutions of cDNAs. We verified the specificity of the amplification by dissociation curve analysis, gel electrophoresis and sequencing of PCR products. We used a single 96 deep-well plate per gene to PCR amplify samples of a given replicate, the F252 and MBS controls, one negative control (without cDNA) to verify that there was no genomic DNA contamination. In addition, we amplified the F252 and MBS control with the *ZmGRP1* reference gene in every plate.

We quantified gene expression by the amplification Cycle threshold (C_T). C_T indicates the number of cycles at which $Q_0=Q_{CT}/(1+E)^{CT}$. We first used *ZmGRP1* C_T in F252 and MBS controls to evaluate the significance of the effects of the Line (F252, MBS), Year (1, 2) and their interaction, as well as the "deep-well plate effect" (Plate 1-6) confounded with the Gene effect (Table S1). Second, we used *ZmGRP1* C_T of all samples (except controls) to test significance of the Replicate, Progenitor, SAM Status (V, T, R), Organ (SAM, Immature Leaf, Mature Leaf and Sheath) effects and the interactions between Status:Organ (Table S2). In order to account for differences in initial cDNA quantities across samples, we normalized C_T across all samples by *ZmGRP1* C_T values. Resulting normalized values (Ratios=R) were used in all subsequent analyses (Table S2).

For all five genes, we employed the following linear regression model that decomposed variations of R into 4 fixed effects, an interaction effect and a residual:

bioRxiv preprint first posted online Nov. 5, 2018; doi: http://dx.doi.org/10.1101/461947. The copyright holder for this preprint (which was not peer-reviewed) is the author/funder, who has granted bioRxiv a license to display the preprint in perpetuity.
It is made available under a CC-BY-NC-ND 4.0 International license.

$R_{ijkl} = Rep_i + Prog_j + Status_k + Organ_l + Status_k \times Organ_l + e_{ijkl}$

with Rep_i =1,2,3; $Prog_j$ = FE, FL, FVL, ME, ML; $Status_k$ =V, T, R; $Organ_l$ =M, IL, ML, S; and e_{ijkl} the residual. We calculated adjusted means after correcting for Rep effect, and 95% confidence intervals. Finally, we performed contrasts to compare adjusted means of all 60 pairwise combinations of Progenitor (5) x Status (3) x Organ (4). We retained as significant P-values<1/1000 which was just above the Bonferroni threshold.

RNA sequencing, data filtering and mapping.

We performed RNA-Seq using SAM samples from 2012 and one of the 2013 replicate. Because we were limited in the amount (after qRT-PCR reactions) and quality of total extracted RNAs, we were able to obtain sequencing data for a subset of 25 samples (25 libraries, Table 1). Note that we combined Leaf7 and Leaf8 for ME in 2013 in a single sample. In brief from 2.5 to 5µg of total RNA, mRNA was isolated with two rounds of polyA purification, fragmented, converted to cDNA, and PCR amplified according to the Illumina RNA-Seq protocol (Illumina, Inc. San Diego, CA). Oriented cDNA libraries were constructed and 51 bp single-reads sequences were generated using the Illumina Genome Analyzer II (San Diego, CA) at the high throughput sequencing platform of IMAGIF (Gif-sur-Yvette). Illumina barcodes were used to multiplex the samples.

From raw reads, we retrieved Illumina adapters using the software Cutadapt 1.2.1 (Martin 2011) with the following parameters: *count=5 ; minimum length=10 ; length overlap=3* . We trimmed low quality reads by imposing 3 consecutive bases at the 3' end with a score of >20 and discarding reads with a sequence length after trimming <25 pb. We filtered reads with a perfect match against maize rRNAs. We mapped the resulting reads (trimmed, filtered and uniquely-mapped) against the maize reference genome v3

bioRxiv preprint first posted online Nov. 5, 2018; doi: http://dx.doi.org/10.1101/461947. The copyright holder for this preprint (which was not peer-reviewed) is the author/funder, who has granted bioRxiv a license to display the preprint in perpetuity.
It is made available under a CC-BY-NC-ND 4.0 International license.

(http://ftp.maizesequence.org/) using Tophat (Trapnell et al., 2009) that accounts for exons-introns junctions using end-to-end alignment with the following parameters adapted to shorts reads with a short seed (L15) and with very sensitive parameters (-i): *--b2-D 25 --b2-R 3 --b2-N 0 --b2-L 15 --b2-i S,1,0.5 --b2-n-ceil L,0,0.5*. We provided transcript annotations during the reads mapping.

From the resulting sam files we retrieved the uniquely mapped reads imposing a filter on read containing NH:i:1. We used coverageBed with the –split option where bed entries are treated as distinct intervals, and retained reads mapped to exons only (as described in Zea_mays.AGPv3.22.gtf, http://ftp.maizesequence.org/). We parsed the resulting file to determine the number of exons, the transcript length, the number of counts (raw counts) per transcript and their coverage (number of bases covered by at least one read). We used the raw counts of the longest transcript of each gene to perform the rest of the analyses.

RNA-Seq filtering and normalization.

We used the standard procedures proposed by DESeq2 v1.14.1 (Love et al., 2014) for filtering and normalization. We computed libraries size factors after data filtering to eliminate transcripts with less than one count per million reads in half of the libraries. We considered libraries of the same progenitor having the same SAM status albeit different leaf stages as replicates irrespective of the year of experimentation. We applied the following graphical procedures to verify our pipeline: we examined boxplots of the libraries counts distributions to validate the normalization procedure; we evaluated pairwise correlations between replicates both on normal and logarithmic scales; we performed multidimensional scaling (MDS) as suggested to compute pairwise distances between libraries based on the 500 genes with the largest standard deviation among samples, and represented the libraries graphically in a two dimensional space.

bioRxiv preprint first posted online Nov. 5, 2018; doi: http://dx.doi.org/10.1101/461947. The copyright holder for this preprint (which was not peer-reviewed) is the author/funder, who has granted bioRxiv a license to display the preprint in perpetuity.
It is made available under a CC-BY-NC-ND 4.0 International license.

Detection of Differentially Expressed genes (DE genes) from RNA-Seq data.

In order to identify Differential Expressed genes (thereafter, DE genes), we used the DESeq2 package (Love et al., 2014) along with its internal filtering procedure that chooses the filtering threshold from the average gene expression of DE genes. The overdispersion parameters were estimated from the whole data set. We next performed pairwise comparisons between libraries by computing contrasts sequentially and determining the associated P-values for each transcript after correction for multiple testing (Benjamini and Hochberg, 1995).

In our experimental setting, a Progenitor represents an early or a late genotype (E, L, or VL) issued from one of the two Lines (F or M). In addition, we sampled three SAM Status (V, T, R) and performed two Years of field experimentation. Altogether, we tested the following contrasts: (1) one comparison between average Year effects across all samples; (2) one comparison between average Line effects across all samples ; (3) three comparisons between early and late Progenitors of each DSE regardless of the SAM Status (FE vs FL, FE vs FVL, ME vs ML); (3) three comparisons between Lines regardless of the SAM Status considering either early and late Progenitors alternatively (FE vs ME, FL vs ML, FVL vs ML); (4) three comparisons of SAM Status within each DSE regardless of Progenitors (V vs T, V vs R, T vs R); (5) three comparisons of SAM Status by Progenitor (V vs T, V vs R, T vs R in FE, FL, FVL, ME, ML, respectively). Considering 25 samples and missing combinations of Progenitor x Status x Year (Table 1), we performed a total of 27 contrasts. Note that the filtering procedure generated different sets of genes retained for each contrast.

Altogether, our analysis corresponded to the following linear decomposition of the mean expression, $Theta_{ylgs}$:

bioRxiv preprint first posted online Nov. 5, 2018; doi: http://dx.doi.org/10.1101/461947. The copyright holder for this preprint (which was not peer-reviewed) is the author/funder, who has granted bioRxiv a license to display the preprint in perpetuity.
It is made available under a CC-BY-NC-ND 4.0 International license.

$$Theta_{ylgs} = Year_y + Line_l + Line(Progenitor)_{lg} + Status(Line)_{sl} + Status(Line(Progenitor))_{slg}$$

We determined the number of Differentially Expressed (DE) genes in each contrast. We next considered as DE genes the ones that were detected as differentially expressed in at least one contrast. From the normalised counts, we determined for each DE gene its average expression per Progenitor per Status, corrected for the Year effect using a linear model. We further normalised average gene expression by the overall mean, so that a negative value corresponds to under-expression, and a positive value to over-expression.

Gene clustering from differential expression patterns.

We performed a Principal Component analysis (PCA) using normalised average gene expression of DE genes, after discarding those displaying a Year or Line effect only, or both. Principal components were defined as linear combinations of genes and allowed projection of Progenitor x Status combinations. We calculated the Pearson correlation coefficient of each gene to the first 13 Principal Components (PCs) and attributed each gene to one PC based on the absolute value of the greatest correlation coefficient among 13. We retained 4 lists of DE genes corresponding to the 4 first PCs and built independent heat maps after ordering genes according to their correlation coefficient – from positive to negative correlations.

Functional analysis of DE genes.

We conducted a functional annotation of DE genes using the MapMan (http://mapman.gabipd.org/web/guest/mapman) and Kegg Ontology level 1, 2 and 3 (https://www.genome.jp/kegg/ko.html). We reduced the number of functional categories by reassigning each of the 226 Mapman categories to 36 Mapman categories, and each Kegg levels 2 and 3 to 24 Kegg pathways, corresponding to the following five high-level kegg

bioRxiv preprint first posted online Nov. 5, 2018; doi: http://dx.doi.org/10.1101/461947. The copyright holder for this preprint (which was not peer-reviewed) is the author/funder, who has granted bioRxiv a license to display the preprint in perpetuity.
It is made available under a CC-BY-NC-ND 4.0 International license.

categories (Kegg level 1): Metabolism, Genetic Information processing, Environmental Information processing, Cellular processes, Organismal systems. We next used a bilateral exact Fisher to test for categories' enrichment/depletion for DE genes belonging to the 4 first PCs, DE genes within the Selection category and genes differentially expressed between lines most of which were discarded from the PCA analysis. We computed the standardized residuals as a standardized measure of the difference between the observed and expected counts.

bioRxiv preprint first posted online Nov. 5, 2018; doi: http://dx.doi.org/10.1101/461947. The copyright holder for this preprint (which was not peer-reviewed) is the author/funder, who has granted bioRxiv a license to display the preprint in perpetuity.
It is made available under a CC-BY-NC-ND 4.0 International license.

SUPPLEMENTAL MATERIAL.

Figure S1. Pedigree of the progenitors in the F252 and MBS DSEs.

Figure S2. SAM Status of pooled samples for Year 1 and Year 2 and by Progenitor.

Figure S3. Distribution of normalized counts with 25 and 75 quantiles for the 25 RNA-seq libraries.

Figure S4. Venn Diagram of DE genes included in the Selection category. The category was further divided into DE genes selected in F252 between FE and FL [SelF], between FE and FVL [SelF], within Status x Progenitor interactions between either FE and FL or FE and FVL [SelF]|[StatusProg], and DE genes selected in MBS [SelM].

Figure S5. Schematic representation of maize flowering time pathway.

Figure S6. Correlations between levels of expression determined by qRT-PCR and RNA-seq for 4 candidate genes.

Supplementary tables are available at: 10.6084/m9.figshare.7271399.

Table S1. Sequencing and mapping statistics.

Table S2. Raw counts for the longest transcript of 39,066 gene in all 25 libraries.

Table S3. Number of Differentially Expressed (DE) genes in 27 contrasts.

Table S4. List of Differentially Expressed genes (12,754) with average gene expression and standard deviation.

Table S5. List of 71 flowering time genes in maize and overlap with Differentially Expressed genes. (continued) List of 2001 Female and/or Male Flowering Time candidates in maize and overlap with Differentially Expressed genes.

Table S6. Enrichment tests of Mapman categories and Kegg pathways for DE genes.

Table S7: Expression of the reference gene *ZmGRP1* as measured by Ct in F252 and MBS controls.

bioRxiv preprint first posted online Nov. 5, 2018; doi: http://dx.doi.org/10.1101/461947. The copyright holder for this preprint (which was not peer-reviewed) is the author/funder, who has granted bioRxiv a license to display the preprint in perpetuity.
It is made available under a CC-BY-NC-ND 4.0 International license.

Table S8: Expression of the reference gene *ZmGRP1* and 5 candidate genes as measured by CT in all samples, and normalized expression in candidates.

Table S9: Significance of effects for each of the 5 candidate genes as determined by linear regression.

ACCESSION NUMBERS.

RNA-seq data were deposited in the Gene Expression Omnibus database from the National Center for Biotechnology Information under accession number XXX.

ACKNOWLEDGMENTS.

This work has benefited from the facilities and expertise of the high throughput sequencing platform of IMAGIF (Centre de Recherche de Gif, www.imagif.cnrs.fr), with appreciated advice from Delphine Naquin, Maud Sylvain and Yan Jaszczyszyn. We are grateful to Coraline Linguat, Betty Leitte, and Hélène Corti for their technical assistance; and to Peter Morrell for helpful discussion.

bioRxiv preprint first posted online Nov. 5, 2018; doi: http://dx.doi.org/10.1101/461947. The copyright holder for this preprint (which was not peer-reviewed) is the author/funder, who has granted bioRxiv a license to display the preprint in perpetuity.
It is made available under a CC-BY-NC-ND 4.0 International license.

TABLES.

Table 1. Meristem Status (V, T, R) and timing of floral transition by Progenitor, Year and developmental stage as determined from pooled samples.

Prog[a]	Year[b]	Leaf6[c]	Leaf7[c]	Leaf8[c]	Leaf9[c]	Leaf10[c]	Leaf11[c]	Leaf12[c]
FE	1	$\underline{V}_{30}$	$\underline{V}_{31}$	$\rightarrow\underline{T}_{19}$	$\underline{R}_{20}$			
FE	2	V_{30}	$\underline{V}_{30}$	$\rightarrow\underline{T}_{20}$	R_{21}			
FL	1	$\underline{V}_{29}$	$\underline{V}_{31}$	$\rightarrow\underline{T}_{24}$	$\underline{R}_{26}$			
FL	2	V_{30}	$\underline{V}_{25}$	$\rightarrow\underline{T}_{21}$	$\underline{R}_{18}$			
FVL	1			$\underline{V}_{34}$	$\rightarrow T_{35}$	T_{19}	$\underline{T}_{24}$	
FVL	2			V_{30}	V_{30}	$\rightarrow\underline{T}_{21}$	$\underline{R}_{21}$	
ME	1		$\underline{V}_{28}$	V_{32}	$\rightarrow\underline{T}_{18}$	T_{25}		
ME	2		$\underline{V}_{30*}$	$\underline{V}_{30*}$	$\rightarrow\underline{T}_{20}$	$\underline{R}_{20}$		
ML	1			V_{32}	V_{32}	$\rightarrow T_{21}$	$\underline{T}_{16}$	
ML	2			V_{30}	V_{30}	$\rightarrow T_{20}$	$\underline{T}_{20}$	$\underline{R}_{20}$

[a]: Progenitors are defined by Line (F=F252, M=MBS) and genotype (E=Early, L=Late, VL=VeryLate)

[b]: Year1=2012, Year2=2013

[c]: Developmental stage (stage) defined as the number (n) of visible leaves (Leafn). Meristem status (V, T, R) was determined by the status of the majority of pooled meristems (number of pooled meristems is indicated in subscript). Floral transition indicated by an arrow is defined as the earliest stage for which the transition stage is reached. Samples used for RNA-Seq are

bioRxiv preprint first posted online Nov. 5, 2018; doi: http://dx.doi.org/10.1101/461947. The copyright holder for this preprint (which was not peer-reviewed) is the author/funder, who has granted bioRxiv a license to display the preprint in perpetuity.
It is made available under a CC-BY-NC-ND 4.0 International license.

underlined. Note that we were unable to obtain RNA-Seq for the ML progenitor at the vegetative state (V).

*: These samples were combined for RNA-Seq

bioRxiv preprint first posted online Nov. 5, 2018; doi: http://dx.doi.org/10.1101/461947. The copyright holder for this preprint (which was not peer-reviewed) is the author/funder, who has granted bioRxiv a license to display the preprint in perpetuity. It is made available under a CC-BY-NC-ND 4.0 International license.

Table 2. Number of Differentially Expressed (DE) genes in 27 contrasts.

Categories [a]	G1 [b]	G2 [b]	#DE genes [c]
[Year]	Year:1	Year:2	3713
[Year]			3713
[Line]	Line:F	Line:M	4709
[Line]	Prog:FE	Prog:ME	5991
[Line]	Prog:FL	Prog:ML	4085
[Line]	ProgFVL	Prog:ML	3785
[Line]			8228
[StatusF]	Status V (Line: F)	Status T (Line: F)	1391
[StatusF]	Status V (Line: F)	Status R (Line: F)	4425
[StatusF]	Status T (Line: F)	Status R (Line: F)	117
[StatusM]	Status V (Line: M)	Status T (Line: M)	2645
[StatusM]	Status V (Line: M)	Status R (Line: M)	1067
[StatusM]	Status T (Line: M)	Status R (Line: M)	0
[StatusF]			4682
[StatusM]			2719
[StatusF]+[StatusM]			6568
[StatusProg]	Status V (Prog: FE)	Status T (Prog: FE)	53
[StatusProg]	Status V (Prog: FE)	Status R (Prog: FE)	487
[StatusProg]	Status T (Prog: FE)	Status R (Prog: FE)	40
[StatusProg]	Status V (Prog: FL)	Status T (Prog: FL)	192
[StatusProg]	Status V (Prog: FL)	Status R (Prog: FL)	1305

bioRxiv preprint first posted online Nov. 5, 2018; doi: http://dx.doi.org/10.1101/461947. The copyright holder for this preprint (which was not peer-reviewed) is the author/funder, who has granted bioRxiv a license to display the preprint in perpetuity.
It is made available under a CC-BY-NC-ND 4.0 International license.

[StatusProg]	Status T (Prog: FL)	Status R (Prog: FL)	302
[StatusProg]	Status V (Prog: FVL)	Status T (Prog: FVL)	266
[StatusProg]	Status V (Prog: FVL)	Status R (Prog: FVL)	396
[StatusProg]	Status T (Prog: FVL)	Status R (Prog: FVL)	3
[StatusProg]	Status V (Prog: ME)	Status T (Prog: ME)	1038
[StatusProg]	Status V (Prog: ME)	Status R (Prog: ME)	451
[StatusProg]	Status T (Prog: ME)	Status R (Prog: ME)	0
[StatusProg]	Status T (Prog: ML)	Status R (Prog: ML)	1
[StatusProg]			2499
[Sel]|[StatusProg]			1646
[SelF]	Prog: FE	Prog: FL	346
[SelF]	Prog: FE	Prog: FVL	576
[SelM]	Prog: ME	Prog: ML	446
[SelF]			748
[SelF]+[SelF]|[StatusProg]			2120
[SelF]+[SelM]			1130
[SelF]+[SelF]|[StatusProg]+[SelM] [d]			2451

[a] : [Year]: Contrasts between Years; [Line]: Contrasts between Lines; [StatusF] and [StatusM]: Contrasts between Status within F and M Line respectively; [SelF] and [SelM]: Contrasts between E and L or VL within F and M Line respectively; [StatusProg]: Contrasts between Status within Progenitor.

[b] : Contrasts were performed between two groups (G1, G2) of libraries.

bioRxiv preprint first posted online Nov. 5, 2018; doi: http://dx.doi.org/10.1101/461947. The copyright holder for this preprint (which was not peer-reviewed) is the author/funder, who has granted bioRxiv a license to display the preprint in perpetuity.
It is made available under a CC-BY-NC-ND 4.0 International license.

[c] : A single gene can be significant in multiple contrasts so that the sum of a given category does not equal the sum of all DE genes for that category. The total number of DE genes for each category after removing this redundancy is shown in shaded rows.

[d] : Within the StatusProg contrasts, we considered the DE genes that were differentially expressed in comparisons among status for Progenitor FE but not for Progenitors FL or FVL and reciprocally, as selected within F Line ([SelF]).

bioRxiv preprint first posted online Nov. 5, 2018; doi: http://dx.doi.org/10.1101/461947. The copyright holder for this preprint (which was not peer-reviewed) is the author/funder, who has granted bioRxiv a license to display the preprint in perpetuity.
It is made available under a CC-BY-NC-ND 4.0 International license.

Table 3. Number of Differentially Expressed (DE) genes correlating best with one of the 4 first Principal Components (PCs) by type. Type includes DE genes, genes of the Selection category (as defined in Table 2, [SelF],[SelM],[SelF]|[StatusProg]); FT_candidates and GWA_candidates (as defined in Table S5).

	DE Genes	Selection	FT_candidates	GWA_candidates
Initial Counts (IC)	NA	NA	70	984
DE genes (% IC)	12,754	2,451	54 (77.1)	294 (29.9)
PC1 (% DE)	3,850 (30.2)	1,134 (46.3)	26 (48.1)	139 (47.3)
PC2 (% DE)	2,388 (18.7)	739 (30.1)	9 (16.7)	53 (18.0)
PC3 (% DE)	522 (4.1)	264 (10.8)	2 (3.7)	12 (4.1)
PC4 (% DE)	278 (2.2)	97 (3.9)	0 (0.0)	0 (0.0)
Total $PC_{1\text{-}4}$ (%DE)	7,038 (55.2)	2,234 (91.1)	37 (68.5)	204 (69.4)

bioRxiv preprint first posted online Nov. 5, 2018; doi: http://dx.doi.org/10.1101/461947. The copyright holder for this preprint (which was not peer-reviewed) is the author/funder, who has granted bioRxiv a license to display the preprint in perpetuity.
It is made available under a CC-BY-NC-ND 4.0 International license.

FIGURE LEGENDS.

Figure 1. Response to selection in the Saclay DSEs during the first 13 generations. Dotted lines represent the average flowering time of each family (days to flowering) plotted against time in generation, after correction for the average year effects. Vertical lines indicate standard deviation within families. Data are taken from (Durand et al., 2015). Plain lines represent the average trends in response to selection for the Early, Late and VeryLate F252 populations and the Early and Late MBS populations.

Figure 2. Multidimensional scaling of normalized counts across all 25 libraries. The top 500 genes (those with the largest standard deviations of expression among samples) were considered.

Figure 3. Heat maps comparisons of differential gene expression across Progenitors and Status for 4 independent sets of DE genes as defined by their correlations to the 4 first Principal Components. PC1 explained 38% of the variation (A), PC2 26% (B), PC3 9% (C) and PC4 7% (D). In diagrams, the legend is the same as in Fig. 2 (circles=F252, triangles=MBS, colours representing the SAM status from vegetative to reproductive).

Figure 4: Adjusted means of log(Expression) across Replicates and 95% CI determined by qRT-PCR for 5 genes *ZMM4* (A&F), *ZCN8* (B&G), *RAP2.7* (C&H), *UBC-like* (D&I), *EiF4A* (E&J) in F252 (A-E) and MBS (F-J). Expression was determined by SAM Status (V=Vegetative, T=Transitioning, R=Reproductive), Organs (Mature part, Immature part and sheath of the last visible leaf, as well as the SAM) and genotypes (Early, Late, VeryLate from left to right in the F252 panel and Early, Late from left to right in the MBS panel).

bioRxiv preprint first posted online Nov. 5, 2018; doi: http://dx.doi.org/10.1101/461947. The copyright holder for this preprint (which was not peer-reviewed) is the author/funder, who has granted bioRxiv a license to display the preprint in perpetuity.
It is made available under a CC-BY-NC-ND 4.0 International license.

Figure 5. Expression patterns of 5 maize flowering time genes and candidates as determined by RNA-seq. Expression was determined by SAM Status (V=Vegetative, T=Transitioning, R=Reproductive) and Progenitor in the two DSEs (F252 and MBS in red and blue colors, respectively) for *KN1* (A), *GA2ox1* (B), *DLF1* (C), *ZMM26* (D), *PIF3.1* (E&F). Expression is measured by average counts across replicates, after correcting for the year effect and vertical bars represent the standard deviation around the mean, obtained after dividing the residual variance estimated by DESeq2 for each gene by the number of replicates.

bioRxiv preprint first posted online Nov. 5, 2018; doi: http://dx.doi.org/10.1101/461947. The copyright holder for this preprint (which was not peer-reviewed) is the author/funder, who has granted bioRxiv a license to display the preprint in perpetuity.
It is made available under a CC-BY-NC-ND 4.0 International license.

LITERATURE CITED.

Abley K, Locke JCW, Leyser HMO (2016) Developmental mechanisms underlying variable, invariant and plastic phenotypes. Annals of Botany **117:** 733-748

Alter P, Bircheneder S, Zhou L-Z, Schlueter U, Gahrtz M, Sonnewald U, Dresselhaus T (2016) Flowering time-regulated genes in maize include the transcription factor ZmMADS1. Plant Physiology **172:** 389-404

Andres F, Coupland G (2012) The genetic basis of flowering responses to seasonal cues. Nature Reviews Genetics **13:** 627-639

Benjamini Y, Hochberg Y (1995) Controllling the false discovery rate - a practical and pwerful approach to multiple testing. Journal of the Royal Statistical Society Series B-Methodological **57:** 289-300

Bolduc N, Hake S (2009) The maize transcription factor KNOTTED1 directly regulates the gibberellin catabolism gene ga2ox1. Plant Cell **21:** 1647-1658

Bortiri E, Chuck G, Vollbrecht E, Rocheford T, Martienssen R, Hake S (2006) ramosa2 encodes a lateral organ boundary domain protein that determines the fate of stem cells in branch meristems of maize. Plant Cell **18:** 574-585

Bouche F, Lobet G, Tocquin P, Perilleux C (2016) FLOR-ID: an interactive database of flowering-time gene networks in *Arabidopsis thaliana*. Nucleic Acids Research **44:** D1167-D1171

Brandenburg J-T, Mary-Huard T, Rigaill G, Hearne SJ, Corti H, Joets J, Vitte C, Charcosset A, Nicolas SD, Tenaillon MI (2017) Independent introductions and admixtures have contributed to adaptation of European maize and its American counterparts. Plos Genetics **13:** e1006666

bioRxiv preprint first posted online Nov. 5, 2018; doi: http://dx.doi.org/10.1101/461947. The copyright holder for this preprint (which was not peer-reviewed) is the author/funder, who has granted bioRxiv a license to display the preprint in perpetuity.
It is made available under a CC-BY-NC-ND 4.0 International license.

Buckler ES, Holland JB, Bradbury PJ, Acharya CB, Brown PJ, Browne C, Ersoz E, Flint-Garcia S, Garcia A, Glaubitz JC, Goodman MM, Harjes C, Guill K, Kroon DE, Larsson S, Lepak NK, Li H, Mitchell SE, Pressoir G, Peiffer JA, Rosas MO, Rocheford TR, Cinta Romay M, Romero S, Salvo S, Sanchez Villeda H, da Silva HS, Sun Q, Tian F, Upadyayula N, Ware D, Yates H, Yu J, Zhang Z, Kresovich S, McMullen MD (2009) The genetic architecture of maize flowering time. Science **325:** 714-718

Burke MK, Dunham JP, Shahrestani P, Thornton KR, Rose MR, Long AD (2010) Genome-wide analysis of a long-term evolution experiment with *Drosophila*. Nature **467:** 587-590

Burke MK, Liti G, Long AD (2014) Standing genetic variation drives repeatable experimental evolution in outcrossing populations of *Saccharomyces cerevisiae*. Molecular Biology and Evolution **31:** 3228-3239

Castelletti S, Tuberosa R, Pindo M, Salvi S (2014) A MITE transposon insertion is associated with differential methylation at the maize flowering time QTL Vgt1. G3-Genes Genomes Genetics **4:** 805-812

Chan YF, Jones FC, McConnell E, Bryk J, Buenger L, Tautz D (2012) Parallel selection mapping using artificially selected mice reveals body weight control loci. Current Biology **22:** 794-800

Chan YF, Marks ME, Jones FC, Villarreal G, Jr., Shapiro MD, Brady SD, Southwick AM, Absher DM, Grimwood J, Schmutz J, Myers RM, Petrov D, Jonsson B, Schluter D, Bell MA, Kingsley DM (2010) Adaptive evolution of pelvic reduction in sticklebacks by recurrent deletion of a Pitx1 enhancer. Science **327:** 302-305

Colasanti J, Coneva V (2009) Mechanisms of floral induction in grasses: Something borrowed, something new. Plant Physiology **149:** 56-62

bioRxiv preprint first posted online Nov. 5, 2018; doi: http://dx.doi.org/10.1101/461947. The copyright holder for this preprint (which was not peer-reviewed) is the author/funder, who has granted bioRxiv a license to display the preprint in perpetuity.
It is made available under a CC-BY-NC-ND 4.0 International license.

Colasanti J, Yuan Z, Sundaresan V (1998) The indeterminate gene encodes a zinc finger protein and regulates a leaf-generated signal required for the transition to flowering in maize. Cell **93:** 593-603

Coneva V, Guevara D, Rothstein SJ, Colasanti J (2012) Transcript and metabolite signature of maize source leaves suggests a link between transitory starch to sucrose balance and the autonomous floral transition. Journal of Experimental Botany **63:** 5079-5092

Danilevskaya ON, Meng X, Selinger DA, Deschamps S, Hermon P, Vansant G, Gupta R, Ananiev EV, Muszynski MG (2008) Involvement of the MADS-Box gene ZMM4 in floral induction and inflorescence development in maize. Plant Physiology **147:** 2054-2069

Dong Z, Danilevskaya O, Abadie T, Messina C, Coles N, Cooper M (2012) A gene regulatory network model for floral transition of the shoot apex in maize and its dynamic modeling. Plos One **7:** e43450

Ducrocq S, Madur D, Veyrieras J-B, Camus-Kulandaivelu L, Kloiber-Maitz M, Presterl T, Ouzunova M, Manicacci D, Charcosset A (2008) Key impact of Vgt1 on flowering time adaptation in maize: Evidence from association mapping and ecogeographical information. Genetics **178:** 2433-2437

Dudley JW, Lambert RJ (1992) 90-generations of selection for oil and protein in maize. Maydica **37:** 81-87

Durand E, Bouchet S, Bertin P, Ressayre A, Jamin P, Charcosset A, Dillmann C, Tenaillon MI (2012) Flowering time in maize: Linkage and epistasis at a major effect locus. Genetics **190:** 1547-1562

bioRxiv preprint first posted online Nov. 5, 2018; doi: http://dx.doi.org/10.1101/461947. The copyright holder for this preprint (which was not peer-reviewed) is the author/funder, who has granted bioRxiv a license to display the preprint in perpetuity.
It is made available under a CC-BY-NC-ND 4.0 International license.

Durand E, Tenaillon MI, Raffoux X, Thepot S, Falque M, Jamin P, Bourgais A, Ressayre A, Dillmann C (2015) Dearth of polymorphism associated with a sustained response to selection for flowering time in maize. BMC Evolutionary Biology **15:** 103

Durand E, Tenaillon MI, Ridel C, Coubriche D, Jamin P, Jouanne S, Ressayre A, Charcosset A, Dillmann C (2010) Standing variation and new mutations both contribute to a fast response to selection for flowering time in maize inbreds. BMC Evolutionary Biology **10:** 2

Gage JL, Jarquin D, Romay C, Lorenz A, Buckler ES, Kaeppler S, Alkhalifah N, Bohn M, Campbell DA, Edwards J, Ertl D, Flint-Garcia S, Gardiner J, Good B, Hirsch CN, Holland J, Hooker DC, Knoll J, Kolkman J, Kruger G, Lauter N, Lawrence-Dill CJ, Lee E, Lynch J, Murray SC, Nelson R, Petzoldt J, Rocheford T, Schnable J, Schnable PS, Scully B, Smith M, Springer NM, Srinivasan S, Walton R, Weldekidan T, Wisser RJ, Xu W, Yu J, de Leon N (2017) The effect of artificial selection on phenotypic plasticity in maize. Nature Communications **8:** 1348

Gervasi DDL, Schiestl FP (2017) Real-time divergent evolution in plants driven by pollinators. Nature Communications **8:** 14691

Goldringer I, Prouin C, Rousset M, Galic N, Bonnin I (2006) Rapid differentiation of experimental populations of wheat for heading time in response to local climatic conditions. Annals of Botany **98:** 805-817

Good BH, McDonald MJ, Barrick JE, Lenski RE, Desai MM (2017) The dynamics of molecular evolution over 60,000 generations. Nature **551:** 45-+

Graves JL, Jr., Hertweck KL, Phillips MA, Han MV, Cabral LG, Barter TT, Greer LF, Burke MK, Mueller LD, Rose MR (2017) Genomics of parallel experimental evolution in *Drosophila*. Molecular Biology and Evolution **34:** 831-842

bioRxiv preprint first posted online Nov. 5, 2018; doi: http://dx.doi.org/10.1101/461947. The copyright holder for this preprint (which was not peer-reviewed) is the author/funder, who has granted bioRxiv a license to display the preprint in perpetuity.
It is made available under a CC-BY-NC-ND 4.0 International license.

Guo L, Wang X, Zhao M, Huang C, Li C, Li D, Yang CJ, York AM, Xue W, Xu G, Liang Y, Chen Q, Doebley JF, Tian F (2018) Stepwise cis-regulatory changes in ZCN8 contribute to maize flowering-time adaptation. Current biology : CB

Hendry AP (2013) Key questions in the genetics and genomics of eco-evolutionary dynamics. Heredity **111:** 456-466

Hung H-Y, Shannon LM, Tian F, Bradbury PJ, Chen C, Flint-Garcia SA, McMullen MD, Ware D, Buckler ES, Doebley JF, Holland JB (2012) ZmCCT and the genetic basis of day-length adaptation underlying the postdomestication spread of maize. Proceedings of the National Academy of Sciences of the United States of America **109:** E1913-E1921

Irish EE, Nelson TM (1991) Identification of multiple stages in the conversion of vegetative to floral development. Development **112:** 891-898

Kumar I, Swaminathan K, Hudson K, Hudson ME (2016) Evolutionary divergence of phytochrome protein function in *Zea mays* PIF3 signaling. Journal of Experimental Botany **67:** 4231-4240

Laehnemann D, Pena-Miller R, Rosenstiel P, Beardmore R, Jansen G, Schulenburg H (2014) Genomics of rapid adaptation to antibiotics: convergent evolution and scalable sequence amplification. Genome Biology and Evolution **6:** 1287-1301

Lamkey KR (1992) 50 years of recurrent selection in the Iowa Stiff Stalk synthetic maize population. Maydica **37:** 19-28

Lehermeier C, Kraemer N, Bauer E, Bauland C, Camisan C, Campo L, Flament P, Melchinger AE, Menz M, Meyer N, Moreau L, Moreno-Gonzalez J, Ouzunova M, Pausch H, Ranc N, Schipprack W, Schoenleben M, Walter H, Charcosset A, Schoen C-C (2014) Usefulness of multiparental populations of maize (*Zea mays* L.) for genome-based prediction. Genetics **198:** 3-16

bioRxiv preprint first posted online Nov. 5, 2018; doi: http://dx.doi.org/10.1101/461947. The copyright holder for this preprint (which was not peer-reviewed) is the author/funder, who has granted bioRxiv a license to display the preprint in perpetuity.
It is made available under a CC-BY-NC-ND 4.0 International license.

Li L, Petsch K, Shimizu R, Liu S, Xu WW, Ying K, Yu J, Scanlon MJ, Schnable PS, Timmermans MCP, Springer NM, Muehlbauer GJ (2013) Mendelian and non-Mendelian regulation of gene expression in maize. Plos Genetics **9(1)**:e1003202

Lopez-Reynoso JD, Hallauer AR (1998) Twenty-seven cycles of divergent mass selection for ear length in maize. Crop Science **38:** 1099-1107

Lorant A, Ross-Ibarra J, M.I. T (2018) Genomics of long- and short- term adaptation in maize and teosinte. PeerJ Preprints 6:e27190v1

Love MI, Huber W, Anders S (2014) Moderated estimation of fold change and dispersion for RNA-seq data with DESeq2. Genome Biology **15(12):** 550-

Maita R, Coors JG (1996) Twenty cycles of biparental mass selection for prolificacy in the open-pollinated maize population golden glow. Crop Science **36:** 1527-1532

Mascheretti I, Turner K, Brivio RS, Hand A, Colasanti J, Rossi V (2015) Florigen-encoding genes of day-neutral and photoperiod-sensitive maize are regulated by different chromatin modifications at the floral transition. Plant Physiology **168:** 1351-1363

Meng X, Muszynski MG, Danilevskaya ON (2011) The FT-Like ZCN8 Gene Functions as a floral activator and is involved in photoperiod sensitivity in maize. Plant Cell **23:** 942-960

Miller TA, Muslin EH, Dorweiler JE (2008) A maize CONSTANS-like gene, conz1, exhibits distinct diurnal expression patterns in varied photoperiods. Planta **227:** 1377-1388

Moose SP, Dudley JW, Rocheford TR (2004) Maize selection passes the century mark: a unique resource for 21st century genomics. Trends in Plant Science **9:** 358-364

Muszynski MG, Dam T, li BL, Shirbroun DM, Hou Z, Bruggemann E, Archibald R, Ananiev EV, Danilevskaya ON (2006) Delayed flowering1 encodes a basic leucine

bioRxiv preprint first posted online Nov. 5, 2018; doi: http://dx.doi.org/10.1101/461947. The copyright holder for this preprint (which was not peer-reviewed) is the author/funder, who has granted bioRxiv a license to display the preprint in perpetuity.
It is made available under a CC-BY-NC-ND 4.0 International license.

zipper protein that mediates floral inductive signals at the shoot apex in maize. Plant Physiology **142:** 1523-1536

Navarro JAR, Wilcox M, Burgueno J, Romay C, Swarts K, Trachsel S, Preciado E, Terron A, Delgado HV, Vidal V, Ortega A, Banda AE, Montiel NOG, Ortiz-Monasterio I, Vicente FS, Espinoza AG, Atlin G, Wenzl P, Hearne S, Buckler ES (2017) A study of allelic diversity underlying flowering-time adaptation in maize landraces (vol 49, pg 476, 2017). Nature Genetics **49:** 970-970

Rodriguez-Verdugo A, Tenaillon O, Gaut BS (2016) First-Step Mutations during Adaptation Restore the Expression of Hundreds of Genes. Molecular Biology and Evolution **33:** 25-39

Roels SAB, Kelly JK (2011) RAPID EVOLUTION CAUSED BY POLLINATOR LOSS IN MIMULUS GUTTATUS. Evolution **65:** 2541-2552

Sakamoto T, Kobayashi M, Itoh H, Tagiri A, Kayano T, Tanaka H, Iwahori S, Matsuoka M (2001) Expression of a gibberellin 2-oxidase gene around the shoot apex is related to phase transition in rice. Plant Physiology **125:** 1508-1516

Salvi S, Sponza G, Morgante M, Tomes D, Niu X, Fengler KA, Meeley R, Ananiev EV, Svitashev S, Bruggemann E, Li B, Hainey CF, Radovic S, Zaina G, Rafalski JA, Tingey SV, Miao G-H, Phillips RL, Tuberosa R (2007) Conserved noncoding genomic sequences associated with a flowering-time quantitative trait locus m maize. Proceedings of the National Academy of Sciences of the United States of America **104:** 11376-11381

Satoh-Nagasawa N, Nagasawa N, Malcomber S, Sakai H, Jackson D (2006) A trehalose metabolic enzyme controls inflorescence architecture in maize. Nature **441:** 227-230

bioRxiv preprint first posted online Nov. 5, 2018; doi: http://dx.doi.org/10.1101/461947. The copyright holder for this preprint (which was not peer-reviewed) is the author/funder, who has granted bioRxiv a license to display the preprint in perpetuity.
It is made available under a CC-BY-NC-ND 4.0 International license.

Sekhon RS, Lin HN, Childs KL, Hansey CN, Buell CR, de Leon N, Kaeppler SM (2011) Genome-wide atlas of transcription during maize development. Plant Journal **66:** 553-563

Sheehan MJ, Farmer PR, Brutnell TP (2004) Structure and expression of maize phytochrome family homeologs. Genetics **167:** 1395-1405

Swanson-Wagner R, Briskine R, Schaefer R, Hufford MB, Ross-Ibarra J, Myers CL, Tiffin P, Springer NM (2012) Reshaping of the maize transcriptome by domestication. Proceedings of the National Academy of Sciences of the United States of America **109:** 11878-11883

Takacs EM, Li J, Du C, Ponnala L, Janick-Buckner D, Yu J, Muehlbauer GJ, Schnable PS, Timmermans MCP, Sun Q, Nettleton D, Scanlon MJ (2012) Ontogeny of the Maize Shoot Apical Meristem. Plant Cell **24:** 3219-3234

Teixeira JEC, Weldekidan T, de Leon N, Flint-Garcia S, Holland JB, Lauter N, Murray SC, Xu W, Hessel DA, Kleintop AE, Hawk JA, Hallauer A, Wisser RJ (2015) Hallauer's Tuson: a decade of selection for tropical-to-temperate phenological adaptation in maize. Heredity **114:** 229-240

Tenaillon O, Rodriguez-Verdugo A, Gaut RL, McDonald P, Bennett AF, Long AD, Gaut BS (2012) The Molecular Diversity of Adaptive Convergence. Science **335:** 457-461

Teotonio H, Estes S, Phillips PC, Baer CF (2017) Experimental Evolution with *Caenorhabditis* Nematodes. Genetics **206:** 691-716

Thornsberry JM, Goodman MM, Doebley J, Kresovich S, Nielsen D, Buckler ES (2001) Dwarf8 polymorphisms associate with variation in flowering time. Nature Genetics **28:** 286-289

bioRxiv preprint first posted online Nov. 5, 2018; doi: http://dx.doi.org/10.1101/461947. The copyright holder for this preprint (which was not peer-reviewed) is the author/funder, who has granted bioRxiv a license to display the preprint in perpetuity.
It is made available under a CC-BY-NC-ND 4.0 International license.

Trapnell C, Pachter L, Salzberg SL (2009) TopHat: discovering splice junctions with RNA-Seq. Bioinformatics **25:** 1105-1111

Turner CB, Marshall CW, Cooper VS (in press) Parallel genetic adaptation across environments differing in mode of growth or resource availability. Evolution letters

Vollbrecht E, Springer PS, Goh L, Buckler ES, Martienssen R (2005) Architecture of floral branch systems in maize and related grasses. Nature **436:** 1119-1126

Yang Q, Li Z, Li WQ, Ku LX, Wang C, Ye JR, Li K, Yang N, Li YP, Zhong T, Li JS, Chen YH, Yan JB, Yang XH, Xu ML (2013) CACTA-like transposable element in ZmCCT attenuated photoperiod sensitivity and accelerated the postdomestication spread of maize. Proceedings of the National Academy of Sciences of the United States of America **110:** 16969-16974

bioRxiv preprint first posted online Nov. 5, 2018; doi: http://dx.doi.org/10.1101/461947. The copyright holder for this preprint (which was not peer-reviewed) is the author/funder, who has granted bioRxiv a license to display the preprint in perpetuity.
It is made available under a CC-BY-NC-ND 4.0 International license.

Figure 1. Response to selection in the Saclay DSEs during the first 13 generations. Dotted lines represent the average flowering time of each family (days to flowering) plotted against time in generation, after correction for the average year effects. Vertical lines indicate standard deviation within families. Data are taken from (Durand et al., 2015). Plain lines represent the average trends in response to selection for the Early, Late and VeryLate F252 populations and the Early and Late MBS populations.

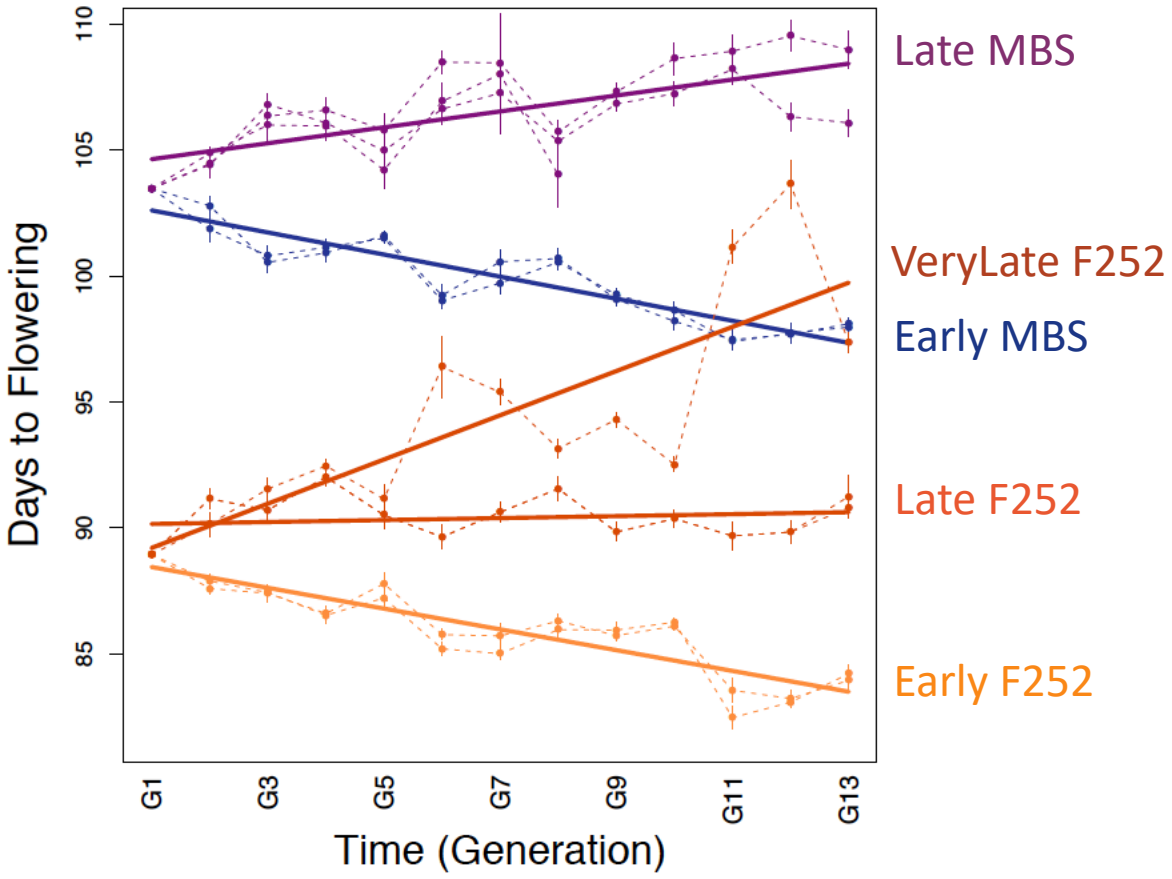

Figure 2. Multidimensional scaling of normalized counts across all 25 libraries. The top 500 genes (those with the largest standard deviations of expression among samples) were considered.

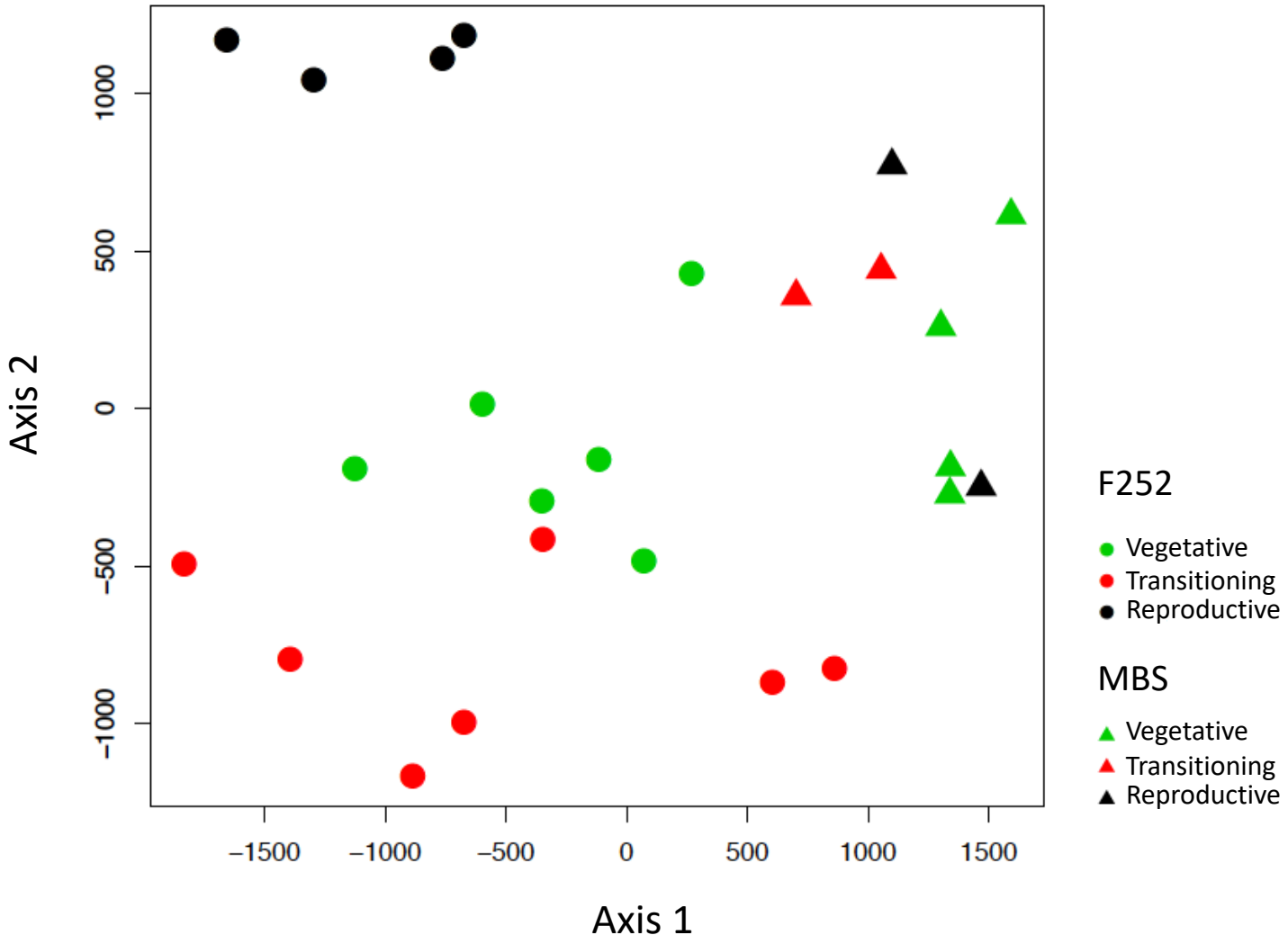

Figure 3. Heat maps comparisons of differential gene expression across Progenitors and Status for 4 independent sets of DE genes as defined by their correlations to the 4 first Principal Components. PC1 explained 38% of the variation (A), PC2 26% (B), PC3 9% (C) and PC4 7% (D). In diagrams, the legend is the same as in Fig. 2 (circles=F252, triangles=MBS, colours representing the SAM status from vegetative to reproductive).

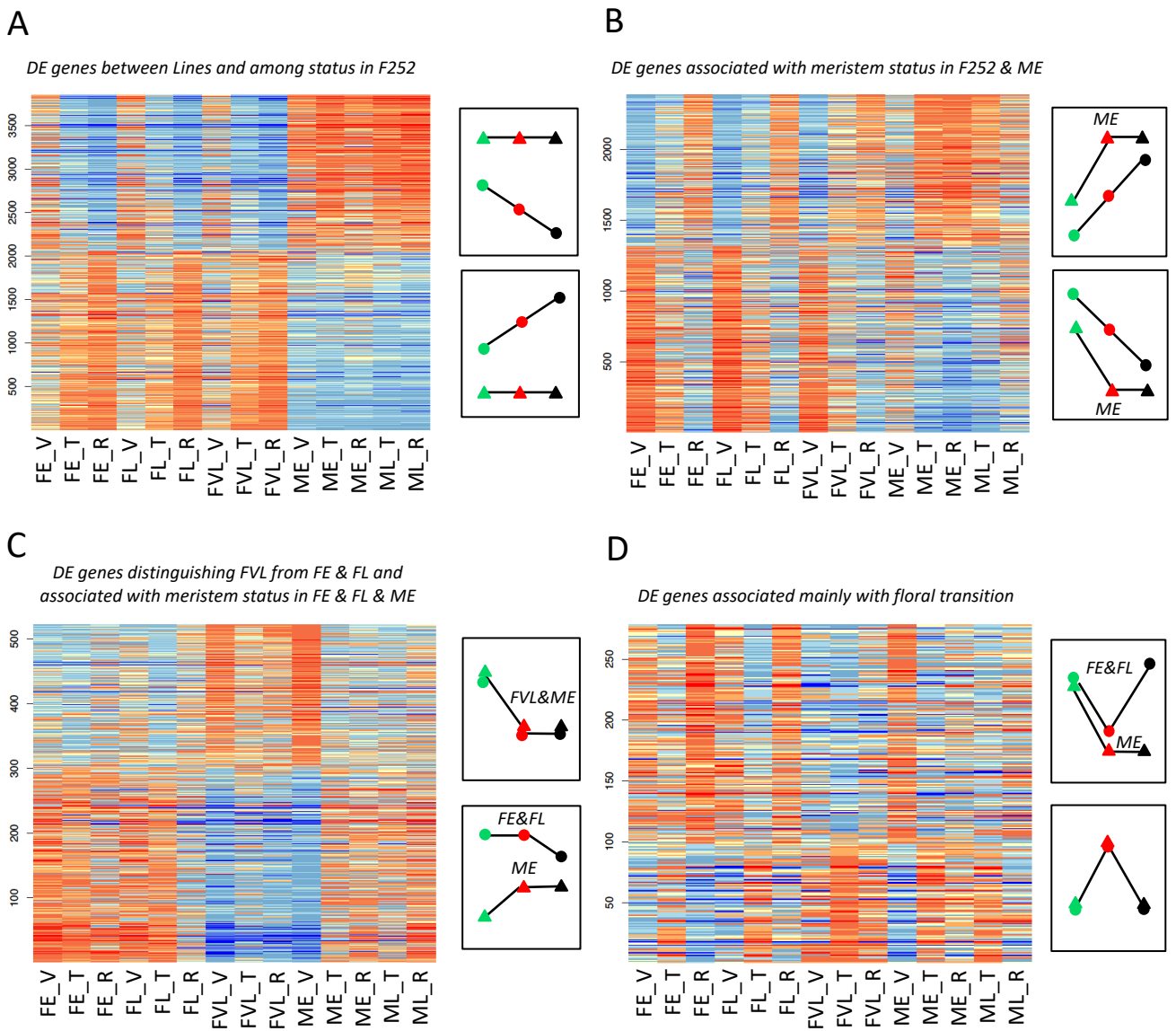

Figure 4: Adjusted means of log(Expression) across Replicates and 95% CI determined by qRT-PCR for 5 genes *ZMM4* (A&F), *ZCN8* (B&G), *RAP2.7* (C&H), *UBC-like* (D&I), *EiF4A* (E&J) in F252 (A-E) and MBS (F-J). Expression was determined by SAM Status (V=Vegetative, T=Transitioning, R=Reproductive), Organs (Mature part, Immature part and sheath of the last visible leaf, as well as the SAM) and genotypes (Early, Late, VeryLate from left to right in the F252 panel and Early, Late from left to right in the MBS panel).

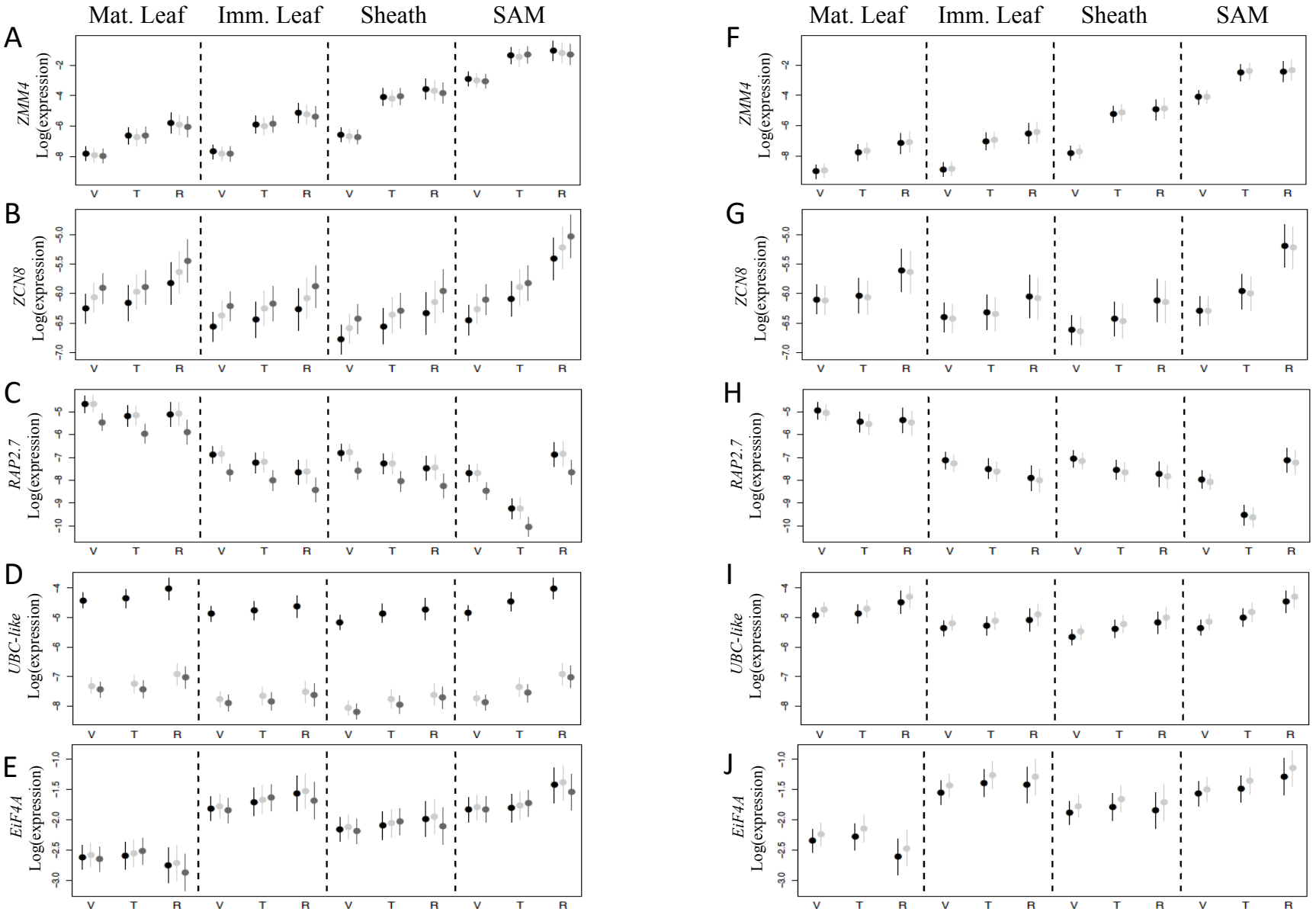

Figure 5. Expression patterns of 5 maize flowering time genes and candidates as determined by RNA-seq. Expression was determined by SAM Status (V=Vegetative, T=Transitioning, R=Reproductive) and Progenitor in the two DSEs (F252 and MBS in red and blue colors, respectively) for *KN1* (A), *GA2ox1* (B), *DLF1* (C), *ZMM26* (D), *PIF3.1* (E&F). Expression is measured by average counts across replicates, after correcting for the year effect and vertical bars represent the standard deviation around the mean, obtained after dividing the residual variance estimated by DESeq2 for each gene by the number of replicates.